Science of the Total Environment 518–519 (2015) 168–188

Contents lists available at ScienceDirect

Science of the Total Environment

journal homepage: www.elsevier.com/locate/scitotenv

The origin of groundwater composition in the Pampeano Aquifer underlying the Del Azul Creek basin, Argentina

M.E. Zabala [a,b,*], M. Manzano [c], L. Vives [b]

[a] Consejo Nacional de Investigaciones Científicas y Técnicas (CONICET), Av. Rivadavia 1917, C1033AAJ Ciudad Autónoma de Buenos Aires, Argentina
[b] Instituto de Hidrología de Llanuras "Dr. Eduardo J. Usunoff", Av. República Italia 780, 7300 Azul, Provincia Buenos Aires, Argentina
[c] Escuela de Ingeniería de Caminos, Canales y Puertos y de Ingeniería de Minas, Universidad Politécnica de Cartagena, P° de Alfonso XIII 52, E-30203 Cartagena, Spain

HIGHLIGHTS

- The work studies the origin of groundwater quality in the shallow Pampeano Aquifer.
- The Pampeano Aquifer is the main support of Argentina's economy.
- Natural groundwater quality is due to a small set of physico-chemical processes.
- The natural groundwater quality is widely modified by human activities.
- Groundwater quality degradation is associated with unplanned use of water and soil.

ARTICLE INFO

Article history:
Received 23 December 2014
Received in revised form 18 February 2015
Accepted 18 February 2015
Available online xxxx

Editor: D. Barcelo

Keywords:
Pampeano Aquifer
Del Azul Creek basin
Groundwater chemistry origin
Isotopic enrichment
Hydrogeochemical modelling

ABSTRACT

The Pampean plain is the most productive region in Argentina. The Pampeano Aquifer beneath the Pampean plain is used mostly for drinking water. The study area is the sector of the Pampeano Aquifer underlying the Del Azul Creek basin, in Buenos Aires province. The main objective is to characterize the chemical and isotopic compositions of groundwater and their origin on a regional scale. The methodology used involved the identification and characterization of potential sources of solutes, the study of rain water and groundwater chemical and isotopic characteristics to deduce processes, the development of a hydrogeochemical conceptual model, and its validation by hydrogeochemical modelling with PHREEQC. Groundwater samples come mostly from a two-depth monitoring network of the "Dr. Eduardo J. Usunoff" Large Plains Hydrology Institute (IHLLA). Groundwater salinity increases from SW to NE, where groundwater is saline. In the upper basin groundwater is of the HCO_3-Ca type, in the middle basin it is HCO_3-Na, and in the lower basin it is $ClSO_4$–NaCa and Cl–Na. The main processes incorporating solutes to groundwater during recharge in the upper basin are rain water evaporation, dissolution of CO_2, calcite, dolomite, silica, and anorthite; cationic exchange with Na release and Ca and Mg uptake, and clay precipitation. The main processes modifying groundwater chemistry along horizontal flow at 30 m depth from the upper to the lower basin are cationic exchange, dissolution of silica and anorthite, and clay precipitation. The origin of salinity in the middle and lower basin is secular evaporation in a naturally endorheic area. In the upper and middle basins there is agricultural pollution. In the lower basin the main pollution source is human liquid and solid wastes. Vertical infiltration through the boreholes annular space during the yearly flooding stages is probably the pollution mechanism of the samples at 30 m depth.

1. Introduction

The study of the origin of the chemical composition of groundwater has many applications, but the most immediate is to use the knowledge gained to set sustainable groundwater management at local, regional and basin scales (Nieto et al., 2005; Manzano et al., 2003, 2008; Shand et al., 2007; Edmunds and Shand, 2008; Custodio and Manzano, 2008; Wendland et al., 2008).

According to Shand et al. (2007), the knowledge of groundwater natural baseline quality is an essential prerequisite for understanding pollution and for imposing regulatory limits. Information on natural groundwater quality should be used as reference conditions in protection programmes and remedial actions. At present, in Latin America there are no laws equivalent to the USA and Canada Water acts, to the European Union Water Framework Directive or to the Directive for the

* Corresponding author at: Consejo Nacional de Investigaciones Científicas y Técnicas (CONICET), Av. Rivadavia 1917, C1033AAJ Ciudad Autónoma de Buenos Aires, Argentina.
E-mail addresses: mzabala@faa.unicen.edu.ar (M.E. Zabala), marisol.manzano@upct.es (M. Manzano), lvives@faa.unicen.edu.ar (L. Vives).

http://dx.doi.org/10.1016/j.scitotenv.2015.02.065
0048-9697/

Protection of Groundwater Quality, but some countries are making conceptual approaches and it is likely that in the near future these laws will exist.

Groundwater chemistry is controlled by: 1 — recharge water chemistry. Groundwater recharge is due mainly to rain infiltration, but in some areas agricultural, livestock and/or urban effluents may also infiltrate to aquifers, usually deteriorating the quality of groundwater. Thus, to understand the origin of groundwater chemistry it is necessary to know the chemical composition of atmospheric and other recharge sources; 2 — reactions between groundwater and the minerals forming the aquifer rocks and sediments. The geological setting provides the main influence on water quality; thus mineralogical information is needed to understand groundwater chemistry; 3 — the effects of the solute transport mechanisms: advection and dispersion. Moreover, the eventual existence of mixing processes may induce changes in groundwater chemistry at different scales from local to regional. In the absence of pollution, groundwater chemistry mainly reflects the mineralogical composition of the rock and sediments and their variability and degree of mineralization depend mainly on the residence time in the aquifer (Edmunds et al., 2003).

The study of groundwater baseline composition has been performed in many aquifers around the world mostly due to national or international requirements derived from the regulations operating in each country (Edmunds and Shand, 2008; Manzano et al., 2003, 2008; Wilcox et al., 2005; Wendland et al., 2008; Daughney et al., 2009; Morgenstern and Daughney, 2012; Krishan et al., 2014). Although Argentina does not have a water law that requires the identification of groundwater baseline, some studies focused on groundwater hydrogeochemistry have been performed in the last decade. Many of these studies focused on the Pampeano Aquifer, which is the largest unconfined aquifer in the country. This aquifer supports the Pampa, a wide plain of 50 million ha which is the most productive rain fed and the strongest economic region of Argentina (Holzman et al., 2013), and the Del Azul Creek basin (DACB) is located in the northeast part of the Pampa. Many of these studies were addressed to identify the main processes originating groundwater chemistry, including natural processes and pollution.

Several authors studied the hydrogeochemical processes providing the Pampeano Aquifer its chemical composition in different places of the Buenos Aires province (Martínez et al., 1998; Logan and Nicholson, 1998; Logan et al., 1999; Martínez and Osterrieth, 1999, 2013; Miretzky et al., 2000, 2001; Heredia et al., 2003; Bonorino et al., 2008; Quiroz Londoño et al., 2008; Kruse et al., 2010; Carol et al., 2012; Manzano and Zabala, 2012). In the DACB basic hydrochemical studies were performed by Sala and Kruse (1987) and Auge and Strelczenia (1990). Since 1996 the Instituto de Hidrología de Llanuras "Dr. Eduardo J. Usunoff" (Large Plains Institute, IHLLA) has been monitoring the chemical quality of the Pampeano Aquifer (Usunoff and Varni, 1995; IHLLA, 1996, 2005, 2008; Usunoff et al., 2003; Zabala, 2009). The studies of groundwater chemical composition and its sources began with Usunoff et al. (1995) and continued with Usunoff and Arias (2004), Zabala et al. (2010, 2011), Zabala (2013), and Zabala et al., (2014).

Due to the favourable climatic conditions, to the existence of fertile soils and of an acceptable transport network, in the last years several governmental institutions have been promoting investment projects related to agriculture and mining in order to encourage the economic development of the DACB region. But these projects are not accompanied by plans for the adequate management of landscape and water resources. In some areas degradation is already observed, mostly located in the lower basin, and it can be associated with unplanned and uncareful use of landscape and water. This situation can worsen in the near future if human pressures intensify.

The main objective of this study is to characterize the chemical and isotopic compositions of groundwater and their origin on a regional scale, focusing on the major and some minor chemical components which are responsible for more than 95% of the chemical composition of groundwater. The study includes the identification of the main sources and processes that explain the chemical composition and the spatial variations of groundwater chemistry. The results will contribute to generate scientific information that will be useful to support the planning and management of groundwater, soil, landscape and economic activities to be applied in the near future in the basin.

2. Study area

The study area comprises the Pampeano Aquifer underlying the DACB, which is located between 36°00′ and 37°20′S and between 60°15′ and 58°45′W. The DACB is part of the Salado River basin and covers an area of 6237 km^2, with some 4500 km^2 corresponding to a typical plain landscape (Migueltorena et al., 2009) (Fig. 1). The catchment spreads between the Tandilia Range System to the southwest and the Salado river valley to the northeast. The Del Azul Creek flows along 160 km from its headwaters nearby Chillar city to the northeast. Nearby Cacharí city the creek is drained by the artificial Channel 11, which flows northeast to reach the Salado River. Before the building of that channel the creek discharged to the Salado River to the north, through a system of shallow lagoons and lowlands (Entraigas et al., 2004).

The Del Azul Creek has two tributaries, the Videla and Santa Catalina creeks. Within the DACB there are other streams, mostly perennial, which do not discharge to the Del Azul Creek streambed; they flow from the Tandilia Range System to the northeastern plain and disappear there mostly by evaporation. The two most relevant ones are La Corina and Cortaderas, which flow almost parallel to the Del Azul Creek. Almost in the whole basin, but especially in the middle and lower sectors, there are abundant permanent and temporal ponds and lagoons occupying the multiple depressions existing in an eolian landscape. Towards the middle basin, and more intensely in the lower one, during humid periods most of the lagoons are connected and almost the whole landscape surface is flooded. In some areas water may flow very slowly and evenly, resulting in surficial ponding water, being evaporation the main evacuation mechanism in them. Those ponds and lagoons are alkaline wetlands (Migueltorena et al., 2009) and the surrounding soils are sodic.

According to Thornthwaite's climatic classification, the climate of the DACB is humid to sub-humid, mesothermal, with little or no water deficiency. Rainfall decreases from north to south. Averaged annual rainfall at the Azul city station of the National Meteorological Survey of Argentina is 914 mm for the period 1901–2012, with the maximum average monthly value in March (118 mm) and the minimum in July (45 mm). Averaged annual temperature at the same station for the period 1966–2003 is 14.5 °C, with the maximum average monthly value in January (21.4 °C) and the minimum in July (7.7 °C). With respect to evapotranspiration, there are a number of works using different methods for different periods and weather stations within the DACB. The most representative work in relation to this study is that of Varni and Usunoff (1999), who calculated an average value for evapotranspiration across the basin of 95.6% of annual rainfall.

Topographically the DACB can be divided into three sections: higher, middle and lower basins (see Fig. 1). Surface slopes average 5% for the upper basin, 0.2% for the lower basin, and 0.5–0.8% in the middle basin (Varni and Usunoff, 1999). The maximum altitude is 300 m asl in the Tandilia Range System; the city of Azul is located at 130 m asl, and the minimum altitude is 60 m asl in the northeast of the basin. Most of the soils in the basin are Argiudolls, Argialbolls, Hapludolls, Natraquolls, Natraqualfs and Paleudolls (SAGyP, 1989). Argic soils have a high infiltration capacity while natric soils have a large range of infiltration capacities, but in all cases they have rates that are much smaller than those of the argic soils. The region has mixed primary productive activities, mainly farming in the south and cattle raising in the north, a feature mainly determined by the type of soils present.

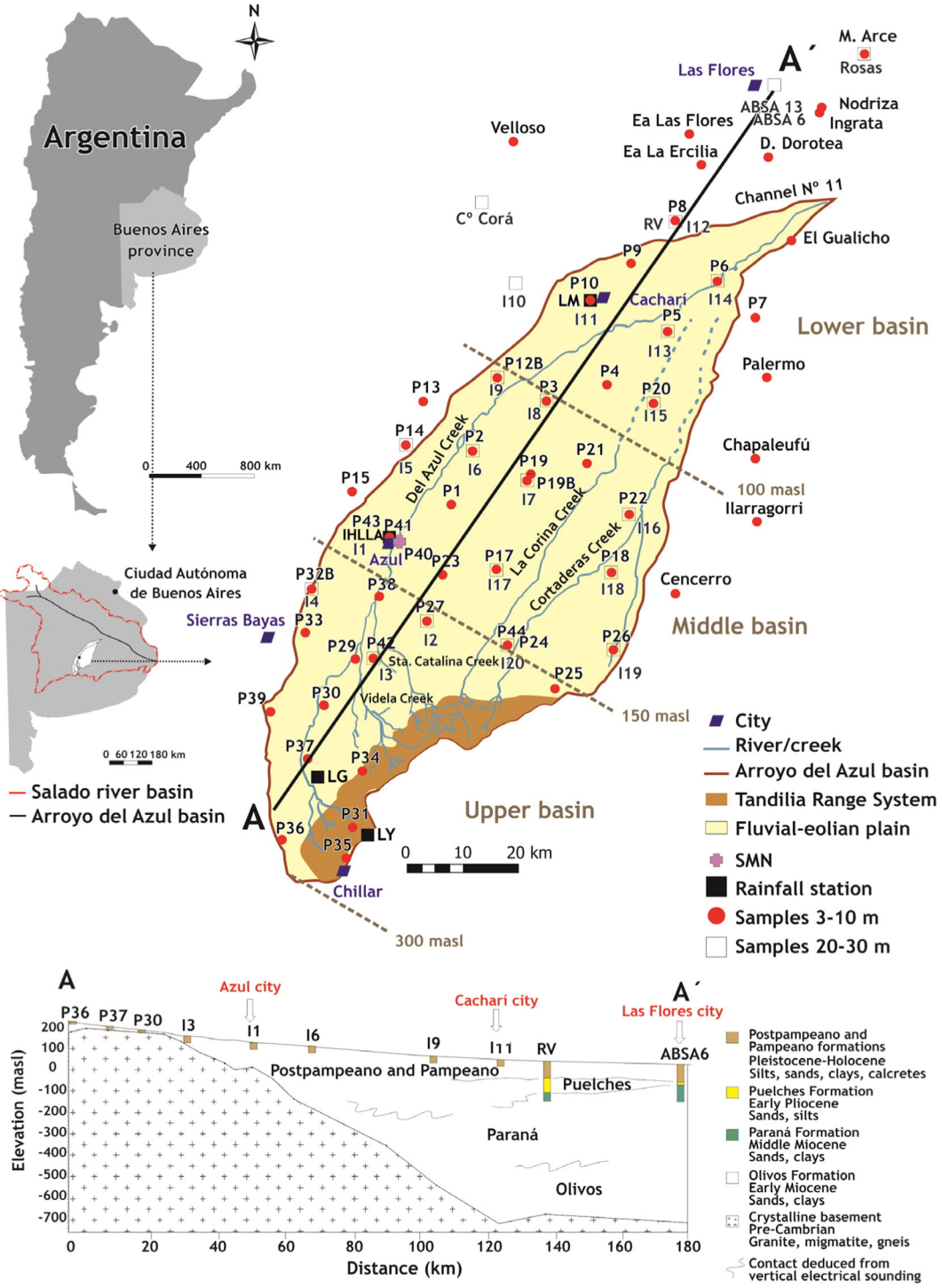

Fig. 1. Location of the study area, Del Azul Creek basin, and illustrative geological cross section. Sampled boreholes and wells and the rain water stations used for the study are also shown.

2.1. Geology and mineralogy

The DACB is a sedimentary alluvial and eolian basin filled up by alluvial and eolian sediments settled since the Pliocene to Recent times over the Precambrian crystalline basement, which crops out in the southwestern border of the basin (Tandilia Range System). The basement is composed of granitic to tonalitic gneisses, migmatites, amphibolites and granitic plutons, with scarce schist and ultramafic rocks (González Bonorino et al., 1956; Teruggi and Kilmurray, 1975, 1980; Dalla Salda et al., 2006). The basement top deepens to the northeast and the sedimentary formations thicken in the same direction, overlapping the basement to the southwest. Thus, in the upper basin the crystalline rocks are quite shallow (<50 m), while in the lower basin they are deeper than 800 m (Fig. 1).

From the upper basin to Azul city, the vertical geological profile is composed from bottom to top of the Pampeano (Pleistocene–Holocene) and Postpampeano (Holocene) formations (Frenguelli, 1950). Both formations, mostly of eolian origin, are composed of silts, sandy silts

and clayey silts with frequent calcretes at shallow depths (Frenguelli, 1955; Fidalgo et al., 1975). These sediments exhibit a marked vertical and horizontal anisotropy due to the alternation of clay and sandy silt layers (Zabala et al., 2006). Between the middle and the lower basin the joint thickness of both units ranges from 130 m near Azul city to 90 m in the northeastern limit of the DACB (Weinzettel et al., 2009). Approximately from Azul city to the northeast, under the Pampeano Formation, appears the Puelches Formation (Early Pliocene). This formation is mostly of alluvial origin and it is formed by yellowish quartz sands, with local thin intercalations of gravels and/or clays (Santa Cruz, 1972), and with the clay abundance increasing towards the top of the formation. To the northeast of the DACB the Puelches Formation is underlain by the Paraná Formation, a marine formation deposited during a broad transgression in Middle to lower Upper Miocene. A shallow sea covered most of eastern, northwestern and central Argentina, reaching as far as Bolivia and the Andean and Patagonian borders. The sediments consist of carbonated (limestone), sandy and argillaceous facies with abundant fossils (Aceñolaza, 2000; Marengo, 2006), and they have original marine (salt) and diluted (brackish) pore water in many places. At the top of the Paraná Formation there is a thin clay layer of coastal and lagoon origin, but under this layer there are very permeable sands and gravels whose connate marine water has been flushed by more recent fresh groundwater. The Paraná Formation is underlain by the Olivos Formation (Oligocene–Miocene), a continental formation of eolian and fluvial origin formed by sands and clays with gypsum (Auge et al., 2002).

The aquifer thickness studied in this work is formed by Pleistocene to Recent sediments which constitute the uppermost cover of the DACB. It is the upper part of the Pampeano Aquifer, which encompasses both Postpampeano and Pampeano sediments. According to Teruggi (1957), González Bonorino (1965), Martínez et al. (1998), Martínez and Osterrieth (1999), Tófalo et al. (2005), Iriondo and Kröhling (2007) and Bonorino et al. (2008), the Pampeano sediments are composed of plagioclase, quartz, potassium feldspar, volcanic glass, calcite, opal, micas and some heavy minerals (magnetite, titanite, ilmenite). Less abundant are pyroxene and amphibole. In the clay size fraction montmorillonite and illite are dominant. A complete mineralogical characterization of Postpampeano sediments within the Salado River basin was performed by Dangavs and Blasi (2002) and Dangavs (2009). They describe the presence of intra-sedimentary gypsum, calcite and dolomite deposits in the lagoons located next to the Salado River.

2.2. Hydrogeology

Groundwater flow direction in the shallowest 30 m of the Pampeano Aquifer is from southwest to northeast, as determined by piezometric surveys using data from the recent IHLLA's two-depths monitoring network tapping the phreatic surface (<10 m) and the piezometric level at 30 m (IHLLA, 2008; Zabala, 2009, 2013). Within these 30 m thickness the vertical hydraulic gradients are very small (Fig. 2) which suggests that groundwater moves mostly horizontally, even if flows are also very small (Zabala et al., 2014). In the upper basin the horizontal hydraulic gradients are larger than 0.002 and the phreatic morphology is concave, with convergent flow into streams; in the middle and lower sectors of the basin the dominant morphology is flat, with horizontal gradients of about 0.001 (Sala and Kruse, 1987). Though the whole aquifer is considered unconfined, due to the marked vertical lithological heterogeneity only the upper part behaves as unconfined, while at 30 depth and below the aquifer behaves as semi-confined (Auge et al., 2002).

Groundwater recharge occurs mainly in autumn and spring. The mean annual recharge for the period 1992–2013 was 202 mm/year, or 17.9% of precipitation, which for this period had an average of 1035 mm/year (Varni et al., 2013). Both the water table and the piezometric levels at 20–30 m depth are generally very shallow, between 2 and 5 m depth. The temporal variation of the piezometric levels at the two study depths reproduces the seasonal pattern of recharge (Zabala, 2013).

2.3. Presence of saline groundwater at regional scale

A marked feature of the northern, flattest part of the DACB and of the terrains beyond the limit of the DACB to the north and northeast is the presence of saline groundwater. The origin of this salinity is well known according to the regional-scale works of several authors at the Salado River basin. Following Auge et al. (2002), Dangavs and Blasi (2002) and Gabellone et al. (2008), among others, the groundwater located in the lower Salado River basin contains NaCl with a salinity that reaches 20 g/L due to several reasons: the low flow velocity that facilitates evaporation, the evaporation and weathering of Postpampeano sediments, and the incidence of marine ingressions that occurred during the Holocene. According to these authors, the presence of high sulphate contents in groundwater could be related to intra-sedimentary gypsum

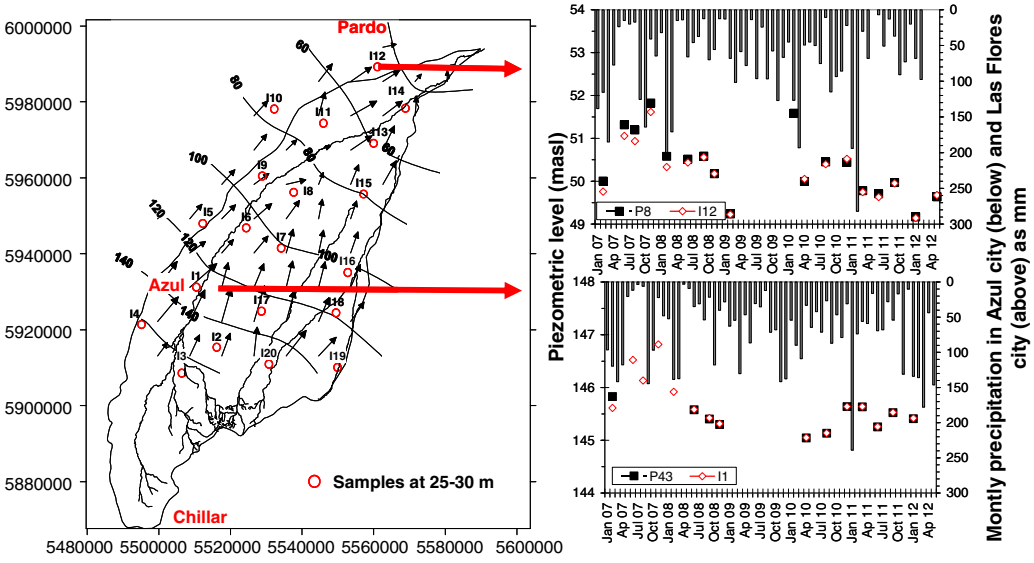

Fig. 2. Left: Piezometric contour lines at 30 m depth according to data from the IHLLA monitoring network. Right: Piezometric hydrographs at two depths, 3–10 m and 30 m, in two representative double-borehole emplacements. From Zabala et al. (2014).

deposits of the upper Pleistocene described within the Salado River basin at a location to the north of the DACB by Dangavs and Blasi (2002).

The presence of this regional body of saline groundwater in the northern part of the DACB has to be considered as a relevant source of salinity by mixing with locally recharged groundwater.

2.4. Human activities relevant for groundwater quality

According to a 2010 census the DACB has a population of 65,280 people, 98.74% coverage of drinking water, and 90.17% access to sewerage services (Oficina de Desarrollo Económico de Azul, personal communication). The major land uses in the DACB and their potential impact on groundwater quality are the following: livestock, agriculture and mining. The main one is livestock (57%), which takes place all around the basin but is more intensive in the middle and lower parts. The lower basin covers a total area of 3,750 km^2 (Argañaráz and Entraigas, 2010), and 78.6% of it is covered by natural soil, 12.6% by crops, and 4.6% by grassland. The rest of the surface is covered by water bodies, forest, streams, and urbanized areas. Here the main activity is cattle raising. During 2010 livestock production reached 550,000 heads and until 2011 there were 25 dairy farms operating. Cattle feeding is carried out by natural pastures (Migueltorena et al., 2009), and dietary supplements are not used. Faeces represent the major pathway for the excretion of many elements such as potassium, calcium, magnesium, nitrogen, sulphur and phosphor, and many trace elements as copper, zinc, manganese, iron, cobalt, selenium, lead and cadmium (Haynes and Williams, 1993).

Agriculture is the second main activity (38%), and it concentrates in the upper and middle basins. Intensive farming began in the 1990s, and the main crops were soy, corn, wheat, barley and sunflower. The main threat for groundwater quality comes from fertilizers, and the most used ones are di-ammonium phosphate, nitrogen and total urea, all of them notable sources of nitrate. The third relevant activity is mining (5%), which concentrates in the very upper basin and exploits granitic and metamorphic rocks. The main risks for groundwater are related to quantity and quality. Though little information exists, a study of Hernández et al. (2002) analysing hydrocarbons, fluorine, arsenic, nitrate, lead, cadmium, zinc and chromium in groundwater, surface water and river sediments did not find significant impacts.

Some activities performed outside the DACB can impact on the quality of groundwater within the basin. Mining is a very important economic activity in the region just nearby the SW border of the DACB, around the small city of Sierras Bayas. The study of Hernández et al. (2002) did not find significant impacts of mining in groundwater and surface water quality. However, from the point of view of the topic of this work, this activity is relevant because it focuses on the exploitation of limestone and dolomite as industrial rocks. These rocks belong to a Precambrian local group called Sierras Bayas, which does not develop into the study area, but the abundant open air exploitations generate carbonated dust which can be distributed by the wind over large areas.

As refers to the rest of the Pampean plain surrounding the DACB, the main activity is farming. But the regional groundwater flow pattern does not favor the transference of potentially polluted groundwater to the studied basin from outside it.

3. Materials and methods

This study involved rain water and groundwater sampling and their physico-chemical and isotopic analyses, as well as soil material sampling and mineralogical and exchange capacity characterization.

Regarding groundwater, a total of seventy-six boreholes were sampled in three field surveys, June 2011, September 2011 and May 2012. Sixty one boreholes belong to the IHLLA double-depth monitoring network. In 20 emplacements there are two boreholes, one with a short screen below the water table (between 3 and 10 m depth, depending on the water table depth and the location in the basin), and the second borehole with a short screen between 20 and 30 m depth. The other 15 boreholes sampled are particular wells and they have depths similar to those of the IHLLA network.

Groundwater samples were taken by pumping after purging. Electrical conductivity (EC), pH and water temperature were measured on-site with a multi-parameter probe and inside a flow-through cell. Alkalinity and air temperature were also measured on-site, alkalinity by acidic titration and temperature with a mercury thermometer. The physicochemical analyses were performed at the IHLLA Laboratory following the methodology proposed by the American Public Health Association (APHA, 2005) and using the following methods: calcium, magnesium, sodium and potassium by flame atomic absorption spectrometry; sulphate by turbidimetry; fluoride by ion selective electrode; chloride by argentometry; nitrate by ultraviolet spectrophotometer screening; carbonate, bicarbonate and alkalinity by titration; EC by conductivity cell; pH by potentiometric electrode; TDS by total dissolved solids dried at 180 °C; hardness by calculation and silica by molybdosilicate method.

Analyses of SiO_2, Al, Cl and Br were performed only in samples of Mayo 2012 at the Geological and Mining Institute of Spain (IGME). SiO_2 was measured by an Autoanalyzer, Al by inductively coupled plasma/mass spectrometry method (ICP/MS), Cl^- and Br^- by ion chromatographic method. All the chemical analyses have ionic balance errors smaller than 10%.

The isotopic data ($\delta^{18}O$ and δ^2H) correspond to samples taken in the boreholes of the IHLLA network but in several surveys: 1999, 2000, 2007 and 2011. The 1999, 2000 and 2007 samples were analysed at the Geochronology and Isotope Geology Institute of Argentina (INGEIS) according to the techniques described by Coleman et al. (1982) and Panarello and Parica (1984); the analytical error was: $\delta^{18}O$: ±0.2‰ and δ^2H: ±1.0‰. The 2010 samples were analysed at the International Atomic Energy Agency (IAEA) by Laser spectroscopy (Lis et al., 2008); the analytical error was $\delta^{18}O$: ±0.1‰ and δ^2H: ±1.0‰. The June 2011 samples were analysed at the Isotope Hydrology Laboratory of Institute of Quaternary and Coast Geology, Mar del Plata University (UNdMP) by laser spectroscopy; the analytical error was $\delta^{18}O$: ±0.3‰ and δ^2H: ±2.0‰. The September 2011 samples were analysed at the Geochronology Laboratory of the Salamanca University (US, Spain) by mass spectrometry under continuous flow; the analytical error was $\delta^{18}O$: ±0.1‰ and δ^2H: ±1.0‰.

As refers to rain water samples, monthly sampling was performed between February 2010 to August 2013 in three sites, one located in the upper basin (Layús — LY station, near Chillar city), a second one placed in the middle basin (IHLLA station, in Azul city) and the third one located in the lower basin (La Madrugada — LM station, in Cacharí city). In September 2011, and for technical problems, the LY sampler was relocated to La Germania (LG station), 16 km far from LY emplacement (see location in Fig. 1). Though rain samples were collected monthly, they were quantitatively integrated into six-month samples and the physico-chemical analyses were performed on those integrated samples. From February 2010 to August 2012 the chemical analyses were performed by the Argentinian Geological and Mining Survey (SEGEMAR), and from August 2012 on they were carried out at the IHLLA Laboratory. All the analyses were performed using standard methods. Isotopic analyses ($\delta^{18}O$ and δ^2H) of rain water samples were performed at the UNdMP.

For the characterization of the aquifer solid material, 15 samples of Pampean loess were collected from the preserved cuttings of 15 boreholes of the IHLLA monitoring network. The sampling sites and depths were selected after a thoughtful screening of the lithological columns available, with the objective of characterizing the different lithologies appearing in the uppermost 30 m of aquifer. Total sample and clay-size fraction mineralogies were analysed by X-ray diffraction at the INTA, according to Thorez (2000) for the total sample and according to Robert and Tessier (1974) for the clay-size fraction. The calcite and dolomite contents were analysed by the Chittick calcimetry method

(Loeppert and Suárez, 1996), and total cationic exchange capacity (CEC) and the contents of exchangeable cations were analysed according to NRCS-USDA (2004). Carbonate content, CEC and exchangeable cations were measured at the Soil Laboratory of the Agronomy Faculty, University of the Centre of Buenos Aires Province (UNCPBA).

The study methodology involved the identification and characterization of potential sources of solutes for groundwater (study of atmospheric deposition, reactions with gases and minerals, pollution processes and mixing of different types of water); deduction of potential physical and chemical processes that produce the observed chemical composition of groundwater and their regional variability (through isotopes and chemical analyses, ionic relation, bivariate analyses, mineral saturation index and mineral stability diagrams); development of a hydrogeochemical conceptual model to explain the processes that may occur during rain water recharge in the upper basin, and during groundwater flow at 30 m depth from the upper basin to the lower basin; and validation of the conceptual models by means of hydrogeochemical modelling, which was performed with the code PHREEQC-Version 3.0 (Parkhurst and Appelo, 1999).

For a clearer writing and reading of the text the signs of the ions have been obviated.

4. Results and discussion

4.1. Identification of potential sources of solutes

4.1.1. Rainfall chemistry

The averaged chemical composition (weighted by rain quantity) of rainwater taken in the three sampling stations during the period 2010–2013 is shown in Table 1. Rainwater from LY–LG and LM stations has very similar composition, while rainwater from the IHLLA station has larger contents of Cl, Na, Ca and SO_4. This is assumed to be the result of dust incorporation to the rain water sampler in an urban environment.

4.1.2. Aquifer solid material

The X-ray diffraction analyses carried out in 15 samples indicate that the most abundant minerals in the uppermost 30 m of Pampeano Aquifer are quartz, plagioclase, potassium feldspar and calcite in the total sample, and illite (I), smectite (S) and the interlayer I/S association in the clay-size fraction. The contents of calcium carbonate are quite homogeneous (Table 2). The contents of magnesium carbonate vary somewhat more and they reach values much larger in the shallower samples than at 30 m depth. The largest calcium carbonate contents were measured in samples from boreholes located in the Azul city (sample I1, middle basin), while the largest magnesium carbonate contents were measured in samples from boreholes located in the lower basin (samples I13 and I14).

CEC values vary between 11 and 27 meq/100 g in the uppermost 11 m of aquifer, and between 23 and 37.8 meq/100 g at 30 m depth (Table 2). At both depths the values increase to the lower basin. The highest CEC values were measured in samples from 20 to 32 m depth located in the middle and lower basins (I5, I9, I15, I13 and I14). The base saturation (BS) values are larger than 100% in all the samples, which suggests that some calcium and magnesium measured come from the dissolution of the solid carbonates. The extractable K is very low in all the samples (Table 2).

4.2. Chemical and isotopic characteristics of groundwater and their origin

4.2.1. Groundwater hydrochemistry

As it was stated in Section 3, the chemical data refers to samples taken in June 2011, September 2011 and May 2012. Though many boreholes were sampled in more than one survey, temporal changes of chemical composition were not observed. Thus, in this work the data from the June 2011 survey, which was the wider one, are preferentially used for those boreholes sampled more than once.

The groundwater chemical types existing in the aquifer thickness studied and their regional evolution are shown in Fig. 3. In the upper basin shallow groundwater (3 to 10 m depth) evolves from HCO_3-Ca/Mg and HCO_3-Mg/Ca types to HCO_3-Na type along the main flow direction. In the middle and lower basins the HCO_3-Na type is the dominant one, though to the northeast other chemical types appear as groundwater salinity increases: SO_4Cl-Na, ClSO_4-Na and Cl–Na types (Zabala et al., 2014). At 20–30 m depth the groundwater chemical types and their regional variability reproduce the characteristics of the shallow layers across the whole basin.

Groundwater salinity increases down gradient from southwest to northeast (Fig. 4). At the uppermost observation depth the EC values vary between 680 and 3110 μS/cm, while at the deeper observation interval they vary between 627 and 5780 μS/cm.

4.2.2. The origin of solutes in groundwater

4.2.2.1. Sources of sodium. Besides the atmospheric supply, the main potential sources of sodium are albite dissolution, cation exchange and mixing with saline groundwater in the lower basin. Almost all the samples studied across the whole DACB and at the two studied depths (3 to 10 m and 20 to 30 m) show a significant sodium excess with respect to chloride (Fig. 5 left). This points to the existence of one or more sources of sodium in addition to the atmospheric one. The potential sources for this sodium excess are albite dissolution, cationic exchange, and leaching of sodium from the soils (mostly in the middle and lower basins). The few samples having a Na/Cl ratio around 1 are low-mineralization samples of the HCO_3-Ca type in the upper basin, that is fresh groundwater recently recharged, and some high-mineralization samples of the Cl–Na type in the lower basin. This suggests that in the lower basin the sources and/or processes increasing both the Cl and Na contents in groundwater are the same. The existence of cationic exchange is confirmed by Fig. 5 (right): all the samples showing a large excess of sodium with respect to chloride also show a joint deficit of calcium and magnesium with respect to bicarbonate and sulphate, and the sodium excess equals the joint deficit of calcium and magnesium. Thus, cationic exchange is the main process controlling the concentrations on these three cations in groundwater at the two study depths and in most of the basin.

With respect to the possible occurrence of albite dissolution, almost all the samples are saturated or oversaturated in this mineral, and only two samples from the upper and middle basins are in equilibrium (Table 1 and Fig. 6). Therefore, this process cannot be a relevant source of sodium, at least in the saturated zone. Chemical information on pore water from the unsaturated zone is not available, but one can argue that if rain water is undersaturated in albite and this mineral is present in the shallow sediments of the aquifer, albite will dissolve. But even if this process occurs during groundwater infiltration, the most relevant source of sodium for groundwater in the major part of the basin is cationic exchange.

In the lower basin there are one or more sources of sodium, chloride and sulphate. Evaporation, a physical process, is a very relevant mechanism increasing the concentration of all the solutes whatever their origin, especially in the lower basin. Besides the effect of evaporation, mixing with saline groundwater in the northern area is the main source of sodium.

4.2.2.2. Sources of sulphate, nitrate and potassium. Besides atmospheric supply, the main potential sources of sulphate are fertilizers, leaching of domestic and agricultural wastewater, and mixing with saline groundwater in the lower basin. Gypsum has not been identified in the soil samples analysed from 3 to 30 m depth and all the groundwater samples are undersaturated in gypsum (data not shown). However, the samples do not

Table 1
Chemical and isotopic compositions of groundwater and rainwater samples (see borehole and rainfall station locations in Fig. 1) and saturation indexes of selected mineral phases.

Name	Elevation (m asl)	Sampling date	Depth (m)	$T^{re\ (f)}$ (°C)	EC $^{(f)}$ (μS/cm)	pH $^{(f)}$	TA $^{(f)}$ (mg/L $CaCO_3$)	Ca (mg/L)	Mg (mg/L)	Na (mg/L)	K (mg/L)	Al (μg/L)	Cl (mg/L)	NO_3 (mg/L)	SO_4 (mg/L)
P1	122	30/06/2011	5.0	16.3	623	7.5	308.0	35.2	19.5	70.9	17.6	NM	10.9	2.9	11.7
P2	114	28/06/2011	5.4	17.1	818	7.5	357.5	35.2	21.7	108.9	22.5	17.0	18.4	10.6	24.9
P3	82	28/06/2011	5.7	16.6	1043	7.4	459.3	36.9	19.9	188.1	20.8	NM	27.2	1.6	37.4
P4	72	27/06/2011	5.7	17.0	1243	7.3	566.5	44.1	17.6	229.4	25.7	NM	26.8	7.6	44.6
P5	54	27/06/2011	5.0	16.9	3120	7.2	827.8	92.2	67.9	460.3	50.8	20.0	247.4	2.6	434.1
P6	48	27/06/2011	5.0	16.8	2380	7.9	649.0	14.3	20.8	419.8	26.3	NM	83.2	2.5	206.2
P7	59	27/06/2011	5.0	17.3	1581	7.6	651.8	19.8	15.3	353.7	24.4	NM	62.5	<1	99.0
P8	59	26/09/2011	5.0	17.1	1512	7.6	705.4	38.5	36.8	321.6	23.1	44.0	44.2	15.0	138.4
P9	54	27/06/2011	5.0	16.2	1472	7.2	409.8	107.5	52.5	141.3	29.7	NM	108.9	4.4	195.9
P10	66	27/09/2011	5.0	16.1	563	7.1	355.9	47.2	21.5	67.7	34.9	23.8	9.2	4.8	31.5
P12B	95	28/06/2011	10.0	16.8	4050	7.3	547.3	55.5	60.2	763.4	18.7	21.0	579.5	28.7	672.4
P13	104	28/06/2011	5.0	16.6	781	7.3	335.5	54.1	21.4	82.6	17.2	NM	21.3	28.8	<1
P14	110	28/06/2011	6.0	16.7	896	7.6	385.0	21.8	10.3	183.4	14.3	18.9	23.2	5.3	33.2
P15	127	29/06/2011	6.0	15.6	719	7.3	354.8	54.0	21.5	79.7	17.5	32.3	8.6	1.4	20.4
P17	128	30/06/2011	6.0	15.5	1033	7.4	453.8	36.2	25.5	163.9	26.9	36.5	43.6	19.9	12.7
P18	118	30/06/2011	6.0	15.9	618	7.1	297.0	70.8	11.9	35.1	18.8	18.8	8.3	<1	11.6
P19	102	27/06/2011	5.0	15.5	699	7.5	332.8	36.3	23.6	88.2	21.5	NM	13.0	2.2	9.1
P19B	105	27/06/2011	10.0	15.6	1228	7.4	508.8	49.6	27.1	199.5	23.6	NM	42.1	26.8	47.7
P20	79	27/06/2011	5.4	16.4	1010	7.4	426.3	46.2	18.4	153.3	20.5	32.5	38.1	<1	46.7
P21	99	27/06/2011	5.0	17.1	738	7.6	346.5	25.2	12.6	113.7	18.2	NM	9.3	4.3	16.0
P22	101	27/06/2011	5.3	16.5	641	7.5	302.5	34.3	17.4	91.9	15.9	16.3	9.7	1.7	11.4
P23	144	30/06/2011	8.0	15.6	720	7.5	343.8	41.6	18.6	74.9	16.2	NM	16.8	4.1	12.9
P24	152	30/06/2011	8.0	15.8	805	7.4	385.0	44.7	25.0	82.3	21.3	NM	16.4	13.6	9.1
P25	166	30/06/2011	10.4	15.4	715	7.5	343.8	48.7	18.3	80.4	22.3	29.3	15.6	15.0	9.7
P26	135	30/06/2011	5.3	16.2	969	7.5	462.0	22.2	18.3	179.3	20.8	NM	27.3	5.4	14.3
P27	159	01/07/2011	8.0	15.1	740	7.5	NM	27.9	22.0	83.4	20.5	43.4	19.3	13.8	11.7
P29	169	29/06/2011	6.2	15.6	771	7.2	357.5	66.9	37.1	42.7	23.6	NM	10.4	44.4	10.9
P30	182	29/06/2011	6.7	14.7	703	7.4	328.6	71.4	35.9	15.7	20.5	98.3	10.8	35.8	9.0
P31	258	29/06/2011	6.6	15.6	684	7.4	356.1	45.7	34.1	59.2	21.8	NM	4.7	2.9	9.1
P32B	161	29/06/2011	6.0	15.3	758	7.4	NM	26.9	33.7	98.5	21.3	18.3	11.1	3.8	<1
P33	187	29/06/2011	6.0	15.2	675	7.4	308.0	66.1	28.0	28.3	24.7	55.6	8.1	31.4	10.3
P34	265	29/06/2011	7.0	15.1	653	7.4	286.0	66.7	34.8	4.0	21.6	11.7	6.8	42.5	12.0
P35	281	29/06/2011	6.5	15.5	1218	7.2	357.5	96.5	64.0	39.3	29.9	NM	92.9	122.4	42.7
P37	207	29/06/2011	8.0	15.3	692	7.3	312.1	70.7	13.8	56.8	18.8	16.2	13.4	36.3	9.0
P38	155	01/07/2011	6.6	15.5	1160	7.7	NM	9.8	13.9	273.8	17.7	NM	20.0	3.4	18.9
P39	216	01/07/2011	3.4	15.0	812	7.2	367.1	86.0	32.0	46.5	22.8	NM	23.0	11.8	22.5
P40	131	29/09/2011	4.7	17.3	1038	7.7	421.7	26.8	12.9	204.5	15.9	NM	24.1	58.4	36.8
P41	134	28/06/2011	4.7	16.6	1510	7.6	657.3	23.7	13.4	349.7	16.3	NM	48.7	25.1	32.3
P42	168	07/01/2011	10.0	15.2	709	7.3	332.8	72.4	34.8	13.1	23.0	13.6	11.9	48.6	9.9

EC = electrical conductivity; TA = total alkalinity; $^{(f)}$ = field measured; NM = not measured; C = calcite, D = dolomite; Al = albite; An = anorthite; KF = K-feldspar; CM = Ca-montmorillonite; I = illite.

Table 1 (*continued*)

Name	Elevation (m asl)	Sampling date	Depth (m)	T^{re} (f) (°C)	EC (f) (μS/cm)	pH (f)	TA (f) (mg/L $CaCO_3$)	Ca (mg/L)	Mg (mg/L)	Na (mg/L)	K (mg/L)	Al (μg/L)	Cl (mg/L)	NO_3 (mg/L)	SO_4 (mg/L)
P43	130	30/06/2011	10.0	15.9	901	8.0	434.5	14.0	3.9	210.5	12.0	NM	15.7	14.4	15.2
P44	159	30/06/2011	10.0	14.6	1044	7.6	441.0	26.2	21.6	161.6	29.3	NM	19.5	47.9	47.3
D. Dorotea	57	24/06/2011	10.0	16.4	2890	7.5	547.8	69.8	65.9	551.5	49.5	NM	382.8	<1	422.4
Ea Las Flores	39	24/06/2011	6.0	17.3	3260	7.5	606.4	62.9	74.9	578.1	35.1	46.4	537.2	8.7	319.0
Ingrata	50	24/06/2011	9.0	19.3	7440	7.3	NM	113.1	189.3	1478	105.7	14.5	2133	<1	1049
La Ercilia	48	10/05/2011	6.7	16.5	5360	7.0	330.0	151.7	224.7	713.9	39.3	NM	1009	3.2	715.2
M Arce	30	10/05/2011	10.0	17.1	867	7.9	330.0	30.8	28.3	95.5	33.3	NM	20.2	16.7	23.5
Velloso	56	10/03/2011	10.0	15.7	1527	7.5	336.0	58.2	39.0	183.5	40.6	14.3	53.0	5.2	124.3
Cencerro	116	16/05/2012	6.0	16.0	1242	7.8	510.6	29.7	16.5	250.4	11.9	16.7	53.0	25.0	73.4
Chapaleofu	93	16/05/2012	9.3	15.7	1050	7.5	432.3	22.0	11.9	218.7	10.8	12.7	53.5	1.9	46.5
El Gualicho	54	05/08/2012	8.8	16.2	2650	7.4	834.8	46.8	66.4	573.3	27.8	15.0	232.1	2.7	385.8
Ilarragorri	96	16/05/2012	5.7	15.9	1046	7.3	377.6	21.6	20.7	182.0	10.6	20.0	71.0	5.1	73.9
Palermo	64	05/08/2012	8.0	16.7	2560	7.4	771.8	21.3	34.7	574.9	19.5	25.1	222.4	7.1	362.9
Nodriza	32	21/06/2011	9.0	15.2	4940	7.3	646.3	96.2	103.0	741.5	104.6	NM	902.2	9.3	619.2
I1	130	30/06/2011	30.0	15.8	899	7.9	396.0	10.3	2.8	182.0	8.1	NM	19.2	8.8	33.6
I2	156	07/01/2011	30.0	15.3	689	7.8	337.2	21.0	6.8	140.9	14.7	51.7	20.1	3.6	13.1
I3	169	07/01/2011	30.0	15.1	656	7.7	308.0	33.6	12.5	99.3	17.0	14.6	17.2	16.2	8.1
I4	167	29/06/2011	30.0	16.0	768	7.6	341.0	31.4	12.3	135.1	17.7	44.7	16.5	11.1	22.9
I5	116	28/06/2011	30.0	16.5	1100	7.5	341.0	33.5	15.5	203.2	21.4	100.0	48.2	6.7	105.5
I6	108	28/06/2011	30.0	16.4	975	7.6	319.0	26.3	11.0	192.8	19.2	22.7	48.8	7.3	65.9
I7	104	27/06/2011	30.0	16.2	916	7.7	327.3	24.1	10.1	182.0	17.8	NM	37.6	4.4	47.6
I8	86	28/06/2011	30.0	16.4	1066	7.5	379.5	29.6	14.6	204.6	20.6	NM	43.3	7.5	61.7
I9	95	28/06/2011	30.0	16.6	2920	7.2	451.0	70.0	36.2	567.9	25.0	12.2	379.5	4.4	377.5
I10	80	28/06/2011	30.0	16.4	1781	7.6	415.3	27.4	20.2	215.2	25.9	23.3	35.9	60.6	78.4
I11	82	28/06/2011	30.0	16.9	1788	7.4	407.0	47.3	26.9	322.0	27.8	30.2	107.8	7.0	277.5
I12	47	27/06/2011	30.0	16.6	2820	7.4	374.0	75.0	65.4	478.5	39.0	13.4	341.0	9.9	574.4
I13	61	27/06/2011	30.0	16.3	3850	7.6	935.0	27.4	29.2	825.9	30.0	23.2	335.2	2.8	502.1
I14	45	27/06/2011	30.0	16.7	6440	7.2	728.8	99.2	84.1	1298	14.3	18.8	754.1	4.2	1279
I15	82	27/06/2011	30.0	16.5	1233	7.6	481.3	22.1	14.1	208.4	20.3	22.0	48.0	3.8	88.6
I16	104	27/06/2011	30.0	16.0	999	7.7	335.5	23.2	12.2	202.8	15.9	12.9	51.7	4.3	61.6
I17	130	30/06/2011	30.0	15.5	780	7.8	352.0	23.8	9.7	152.9	17.8	34.5	23.9	4.3	24.8
I18	121	30/06/2011	30.0	15.8	832	7.8	376.8	18.4	9.0	178.1	16.6	12.4	26.6	4.8	33.8
I19	135	30/06/2011	30.0	15.7	819	7.9	365.8	14.0	6.4	178.8	16.8	NM	23.7	3.8	23.6
I20	159	30/06/2011	30.0	15.5	730	7.6	357.5	27.0	14.1	125.1	22.0	NM	18.2	9.9	4.2
C° Cora	67	10/03/2011	22.7	15.9	1168	8.0	249.0	28.7	18.8	169.0	30.1	15.1	37.3	2.7	102.4
Rosas	30	24/06/2011	23.8	16.7	1070	7.8	335.5	18.8	15.9	212.2	24.4	240.0	50.2	97.7	33.0
ABSA13	40	21/06/2011	30.0	16.9	1437	8.0	517.0	21.3	21.7	315.5	25.8	NM	83.9	21.0	99.5
LY	275	2010–2011	Rainfall	NM	33.5	5.9	10.3	2.2	0.5	1.0	2.7	NM	1.3	1.0	1.0
LG	220	2011–2013	Rainfall												
IHLLA	145	2010–2013	Rainfall	NM	32.9	6.3	9.4	3.3	0.5	1.3	2.1	NM	2.3	0.5	1.4
LM	72	2010–2013	Rainfall	NM	15.6	6.2	9.8	1.4	0.4	0.9	0.7	NM	1.3	0.4	0.8

Table 1 (*continued*)

Name	HCO_3 (mg/L)	Br (mg/L)	SiO_2 (mg/L)	$\delta^{18}O$ (‰ SMOW)	$\delta^{2}H$ (‰ SMOW)	Mineral saturation index						
						C	D	Al	An	KF	CM	I
P1	370.5	NM	68.4	−5.40	−31.00							
P2	456.9	0.1	71.1	−5.80	−35.00	0.02	0.07	1.16	−1.57	2.92	5.57	5.13
P3	585.4	NM	65.8	−5.40	−33.00							
P4	707.2	NM	81.8	−5.80	−33.00							
P5	1082	1.2	68.9	−4.49	−27.62	0.35	0.81	1.68	−1.45	3.18	5.98	5.58
P6	847.5	0.3	62.6	−4.97	−27.88							
P7	815.1	NM	73.1	−6.00	−36.00							
P8	902.7	0.2	67.4	−5.40	−34.38	0.36	0.95	1.85	−1.07	3.15	5.92	5.62
P9	526.3	0.2	72.9	−5.40	−28.00							
P10	434.2	0.1	77.4	−5.84	−35.55	−0.17	−0.47	1.10	−1.41	3.27	6.41	5.80
P12B	716.3	1.7	70.2	−5.11	−28.86	0.01	0.29	1.94	−1.67	2.77	5.78	5.22
P13	427.3	0.3	66.1	−4.92	−23.66							
P14	494.0	0.1	77.1	−5.80	−34.00	0.02	−0.05	1.53	−1.68	2.87	5.36	4.90
P15	459.4	NM	64.0	−4.70	−32.00	0.08	−0.03	1.16	−1.10	2.96	6.26	5.63
P17	560.7	NM	68.2	−5.60	−35.00	0.06	0.18	1.69	−0.96	3.37	6.51	6.08
P18	377.9	0.0	44.6	−4.50	−23.11	−0.08	−0.71	0.13	−1.65	2.32	5.68	4.84
P19	483.1	0.1	68.2	−3.56	−18.16							
P19B	650.5	0.2	71.2	−5.32	−27.93							
P20	537.1	0.2	50.3	−5.01	−25.06	0.10	0.03	1.09	−1.39	2.66	5.72	5.17
P21	440.0	NM	66.0	−5.00	−29.00							
P22	399.5	0.1	61.2	−5.10	−29.00	0.01	−0.04	0.95	−1.65	2.64	5.33	4.84
P23	419.9	NM	61.1	−5.20	−31.62							
P24	486.6	0.1	65.8	−5.90	−34.00							
P25	427.3	NM	67.4	−5.30	−31.00	0.15	0.08	1.26	−1.04	3.17	6.16	5.68
P26	573.0	NM	59.6	−4.90	−35.00							
P27	420.3	0.1	61.2	−6.00	−35.00	−0.05	0.00	1.30	−1.10	3.16	6.23	5.82
P29	434.7	NM	63.6	−5.55	−31.35							
P30	402.6	NM	59.4	−5.60	−31.00	0.19	0.29	0.95	0.05	3.53	7.44	6.90
P31	447.1	0.0	61.3	−6.10	−37.00							
P32B	464.4	0.2	72.0	−4.73	−24.71	−0.10	0.11	1.26	−1.60	3.06	5.88	5.47
P33	387.8	0.1	65.0	−5.80	−36.00	0.17	0.17	1.07	−0.34	3.48	6.97	6.48
P34	365.6	NM	67.4	−5.50	−36.00	0.09	0.10	−0.50	−1.87	2.70	5.32	4.80
P35	437.2	NM	72.7	−5.60	−33.00							
P37	385.3	NM	63.4	−5.90	−35.00	0.12	−0.25	0.85	−1.31	2.84	5.95	5.26
P38	745.0	NM	58.5	−5.60	−34.00							
P39	459.4	NM	61.8	−5.60	−35.00							
P40	514.5	NM	63.5	−5.08	−29.46							
P41	829.9	NM	61.2	−5.75	−33.10							
P42	398.8	NM	62.9	NM	NM	0.15	0.19	−0.09	−1.92	2.62	5.24	4.71

Table 1 (*continued*)

Name	HCO_3^- (mg/L)	Br (mg/L)	SiO_2 (mg/L)	$\delta^{18}O$ (‰ SMOW)	$\delta^{2}H$ (‰ SMOW)	Mineral saturation index						
						C	D	Al	An	KF	CM	I
P43	526.1	0.1	61.0	−4.97	−25.44							
P44	562.0	NM	74.8	−4.90	−28.30							
D. Dorotea	710.9	0.9	55.5	−3.77	−21.85							
Ea Las Flores	753.4	NM	62.2	−4.98	−25.56	0.33	0.99	2.06	−0.83	3.28	6.16	5.93
Ingrata	437.1	4.4	67.2	−4.62	−23.85	0.06	0.62	1.70	−2.14	2.96	4.63	4.63
La Ercilia	804.2	NM	68.4	−4.95	−25.67							
M Arce	466.4	NM	62.0	−5.37	−26.90							
Velloso	615.8	NM	71.0	−5.24	−27.05	0.28	0.61	1.17	−1.98	2.98	5.10	4.83
Cencerro	631.4	0.2	65.3	NM	NM	0.32	0.60	1.49	−1.72	2.62	5.00	4.61
Chapaleofu	549.6	0.2	61.6	NM	NM	0.40	0.75	1.08	−2.46	2.23	3.72	3.51
El Gualicho	1094	1.5	59.9	NM	NM	0.22	0.81	1.66	−1.80	2.81	5.54	5.16
Ilarragorri	465.4	0.3	62.4	NM	NM	0.06	0.32	1.30	−1.86	2.53	4.97	4.59
Palermo	1009	1.6	71.7	NM	NM	−0.07	0.31	2.05	−1.63	3.03	5.98	5.53
Nodriza	1053	NM	NM	−4.16	−23.43							
I1	412.5	0.1	52.9	−5.08	−25.74							
I2	411.4	0.1	59.8	−5.30	−34.00	0.06	−0.16	1.59	−1.04	3.08	5.90	5.49
I3	386.3	NM	60.9	−5.50	−34.00	0.15	0.07	0.78	−2.21	2.48	4.53	4.14
I4	432.2	0.1	64.1	−5.40	−26.89	0.11	0.03	1.51	−1.04	3.09	5.96	5.53
I5	452.0	0.2	63.2	−5.30	−35.00	−0.04	−0.18	2.02	−0.30	3.49	7.02	6.55
I6	429.8	0.2	65.6	−5.00	−34.00	−0.02	−0.18	1.36	−1.74	2.81	5.21	4.81
I7	440.0	0.2	67.1	−5.02	−26.74							
I8	508.8	NM	63.7	−4.80	−29.00							
I9	615.0	1.3	66.5	−5.07	−28.70	0.01	−0.03	1.45	−2.18	2.54	5.24	4.62
I10	528.6	0.2	64.7	−4.72	−26.78	0.02	0.13	1.38	−1.78	2.91	5.29	4.98
I11	533.5	0.4	64.0	−4.81	−26.04	−0.03	−0.07	1.66	−1.30	3.04	6.02	5.54
I12	485.8	0.8	64.6	−5.17	−31.21	0.05	0.27	1.37	−2.13	2.72	4.95	4.62
I13	1093	1.3	59.0	−4.90	−31.59	0.14	0.53	1.81	−2.05	2.82	5.11	4.84
I14	866.4	1.7	68.2	−4.34	−22.54	0.12	0.40	2.11	−1.56	2.60	6.01	5.24
I15	485.8	0.2	55.7	−5.01	−27.14	−0.08	−0.12	1.17	−1.98	2.61	5.03	4.65
I16	464.2	0.6	66.6	−5.30	−30.00	0.11	0.16	1.13	−2.37	2.48	4.35	4.02
I17	437.2	NM	61.8	−4.80	−28.00	0.12	0.07	1.43	−1.42	2.96	5.41	5.09
I18	459.4	0.2	64.6	−4.98	−27.04	0.05	0.02	1.05	−2.47	2.48	4.26	3.96
I19	469.3	NM	63.9	−5.30	−35.00							
I20	444.0	0.1	60.7	−5.60	−33.00							
C° Cora	550.1	0.3	69.4	−5.64	−32.68	0.48	1.01	1.41	−1.66	3.12	4.66	4.70
Rosas	445.0	NM	61.0	−5.18	−27.11	0.04	0.25	2.36	0.19	3.87	7.19	7.03
ABSA13	754.1	NM	NM	−5.07	−27.92							
LY	10.8	NM	NM	−3.39	−19.21							
LG												
IHLLA	12.2	NM	NM	−3.16	−15.27							
LM	9.8	NM	NM	−3.55	−14.17							

Table 2
Cation exchange capacity (CEC), extractable cations, base saturation percentage (% BS), exchangeable sodium percentage (ESP), pH and electrical conductivity (EC) values of Pampeano Aquifer sediments.

Borehole id.	Depth (m)	pH (1:2.5 water)	EC (μS/cm)	CEC (meq/100 g)	Extractable cations (meq/100 g)				BS %	ESP	Calcite %	Dolomite %
					Ca	Mg	K	Na				
Shallow samples												
I20	3	9.20	163	11.3	10.2	6.0	1.3	0.6	160.2	5.3	39.2	1.7
I2	10	8.94	154	21.7	16.4	13.6	2.0	1.2	153.0	5.5	34.4	1.7
I1	6	9.56	297	20.7	23.0	6.6	1.5	2.0	159.9	9.7	44.0	7.9
I12	7	9.63	275	14.6	9.6	7.0	1.5	2.8	143.2	19.2	35.2	0.2
I14	6	9.25	335	27.0	10.2	15.6	2.3	5.3	123.7	19.6	36.0	0.9
I14	11	9.71	552	24.4	20.1	11.4	2.1	7.3	167.6	29.9	38.5	2.8
Deep samples												
I3	22	9.17	174	23.1	23.2	9.5	1.6	1.2	153.7	5.2	36.4	0.9
I1	20	9.66	272	29.7	27.5	7.9	1.8	3.4	136.7	11.5	36.0	1.3
I5	29	9.32	317	35.8	32.6	15.1	1.8	3.0	146.7	8.4	41.0	1.3
I9	29	9.31	439	33.2	31.1	12.5	1.9	4.1	149.4	12.4	40.0	0.5
I15	30	8.86	674	30.2	23.6	13.6	2.1	4.2	144.0	13.9	35.4	0.5
I15	32	8.86	752	29.9	23.7	14.1	2.0	3.9	146.2	13.0	37.5	1.3
I13	20	10.03	388	23.0	13.6	8.3	2.0	7.2	135.2	31.3	36.2	1.7
I13	29	9.63	612	32.6	14.3	14.3	2.1	10.3	125.8	31.6	36.0	0.5
I14	22	9.16	767	37.8	17.6	15.8	2.4	9.2	119.0	24.3	38.0	0.5

represent the whole basin and, moreover, mineralogical analyses of samples from the first 2 m of the aquifer are not available. As mentioned in Section 2.3, Dangavs and Blasi (2002) describe intra-sedimentary gypsum deposits to the north of the Salado River.

Fig. 7a shows that most of the samples from the upper and middle sectors of the basin and at the two study depths have more calcium than sulphate, suggesting that carbonate dissolution, probably driven by cation exchange, is controlling calcium contents. On the contrary, samples from the lower basin have much more sulphate than calcium, suggesting either the existence of a source of sulphate independent of calcium or geochemical limitations for calcium concentrations. On the other hand, there is a good relationship between the evolution of sulphate and chloride contents across the basin, with a notable increase of both towards the lower basin (Figs. 3 and 7b). This means that the main sources and/or processes that increase sulphate and chloride contents in groundwater are the same, which is coherent with the existing knowledge about the origin of water salinity in the lower Salado River basin.

Agriculture and livestock are other potential sources that could add sulphate to groundwater. As it was stated before, the agricultural activity is intense in the upper basin, disperse in the middle one, and inexistent in the lower part. Considering the relationship between sulphate and nitrate contents in groundwater (Fig. 7c) it seems clear that fertilizers are not a relevant source of sulphate even in the upper basin. With respect to the other potential source, in the lower basin livestock activity is intense, and several feed lots have been recently installed in addition to the traditional sparse cattle grazing. The frequent seasonal flooding would facilitate the infiltration of animal waste water through the borehole annular space, carrying pollutants inside the boreholes. Though the very shallow water table would impede that waste water

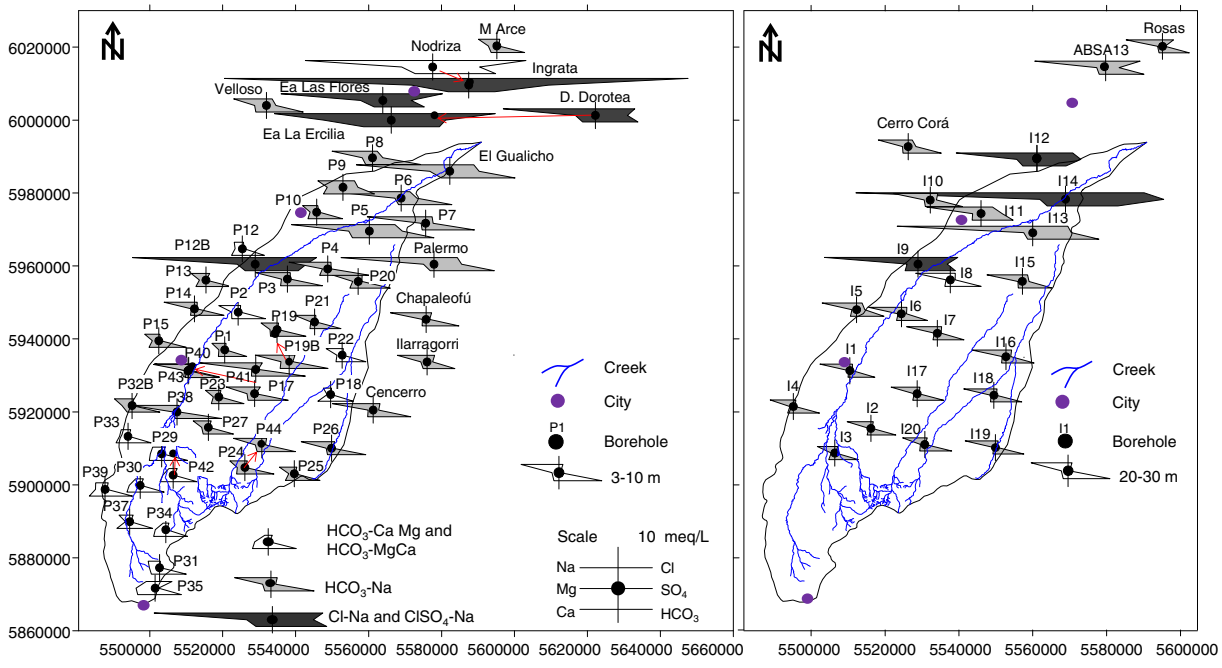

Fig. 3. Groundwater chemical types observed at the two study depths, 3–10 m and 20–30 m.

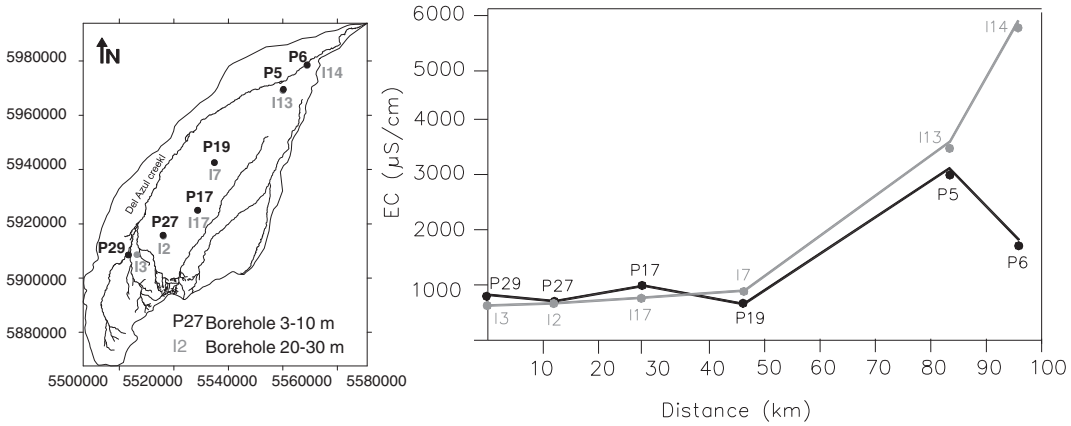

Fig. 4. Electrical conductivity evolution in groundwater from the upper to the lower basin at the two study depths.

reaches significant depths, at least at a regional scale, this polluting mechanism may take place at the borehole scale, favoured by local water depressions induced by pumping in the urban areas.

Thus, the main source of sulphate in groundwater of the upper and middle basins seems to be the concentration by evaporation of atmospheric sulphate supplied by rain water recharge. In the lower basin mixing with saline resident groundwater, together with a more intense evaporation, explain the high sulphate contents of groundwater. The infiltration of animal waste water cannot be discarded as an additional source, but it would contribute to the groundwater sulphate to a less extent than the others.

With respect to the origin of potassium, the potential sources are K-feldspar dissolution, fertilizers, domestic and/or farming wastewater, and evaporation and mixing with saline groundwater in the lower basin. Potassium feldspar (microcline) was identified in the sediments. All the water samples are oversaturated in this mineral (Table 1 and Fig. 6), thus preventing dissolution. However, in the stability diagram of the K-bearing silicates (Fig. 6) all the samples are very close to the microcline–kaolinite stability limit, which means that they approach the conditions for dissolution. A feasible hypothesis to explain this is that the samples studied correspond to geochemically evolved groundwater, not to fresh, recently recharged groundwater. Groundwater in the unsaturated zone and very recent groundwater in the water table would probably have the thermodynamic conditions for K-feldspar dissolution, but groundwater in the first metres of the saturated zone would be already oversaturated.

As regards the possible contribution of fertilizers and waste water, most of the samples in the upper and middle basins show a positive correlation between nitrate and potassium, suggesting that fertilizers and/or domestic and farming waste water are significant sources. The largest contents of potassium are observed in the shallow groundwater of the lower basin (Ingrata, Nodriza, Ea. Las Flores, Doña Dorotea, P5, P8, Ea. La Ercilia, Velloso samples in Fig. 7d), following the sulphate and chloride patterns. In this area animal farming is also a feasible candidate as potassium source, and the low nitrate content in these samples could be explained by the usual reducing conditions of organic-rich animal waste. But as already discussed for sulphate, the high water table position prevents a generalized pollution process by infiltration through the thin unsaturated zone, and the direct transfer of polluted flood water through the annular space would produce borehole-scale pollution. Thus, the main origin for K in the lower basin is evaporation and mixing with saline groundwater.

4.2.2.3. Sources of bicarbonate. The pH values in almost all the groundwater samples is well under 8 (Table 1), thus the major part of the dissolved inorganic carbon occurs as bicarbonate. Bicarbonate contents are quite similar at the two study depths, and they increase from the upper to the lower basin from 450 mg/L to around 1100 mg/L (Table 1). The main

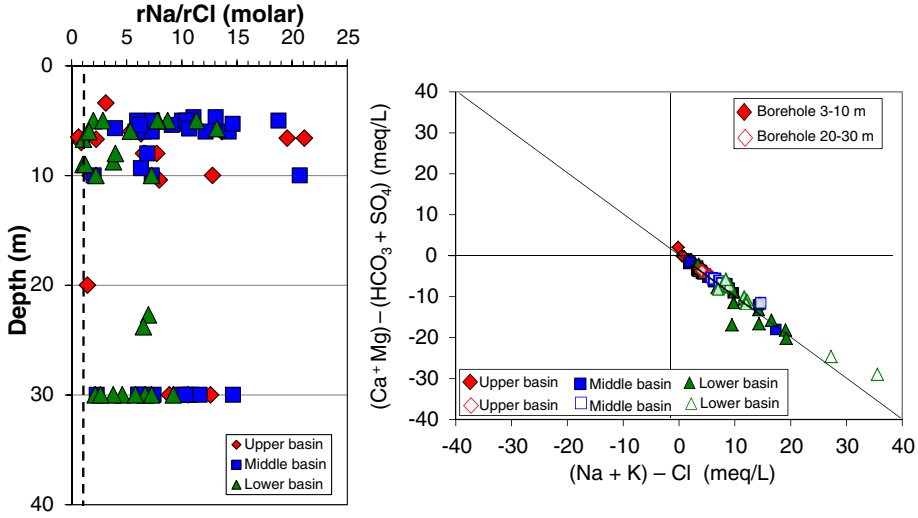

Fig. 5. Left: Values of Na/Cl molar ratio vs. sampling depth. Right: Excess of sodium and potassium vs. joint deficit of calcium and magnesium.

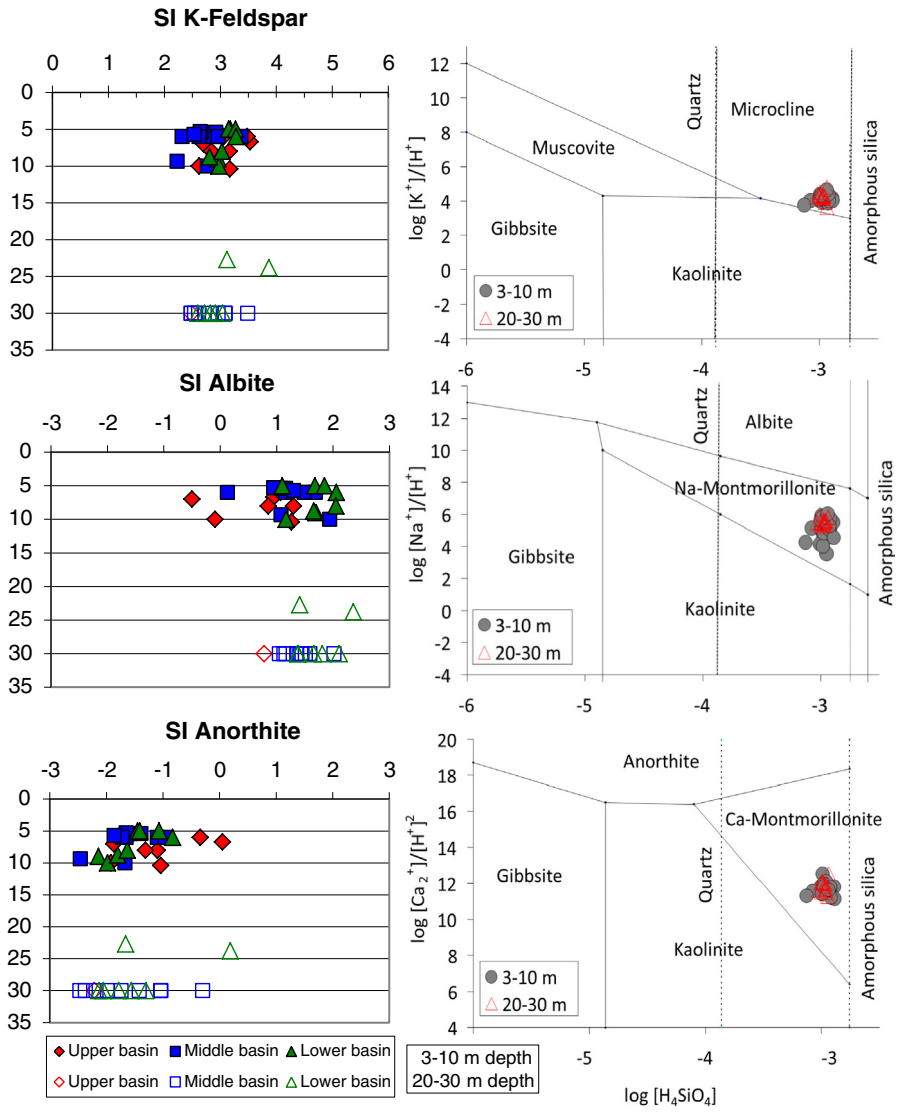

Fig. 6. Left: Saturation indexes of K-feldspar, albite and anorthite vs. depth. Right: Location of the studied samples in the mineral stability diagrams of K-feldspar, albite and anorthite. Modified from Tardy (1971).

potential sources of bicarbonate in groundwater of the DACB are dissolution of 1) edaphic CO_2, 2) carbonate minerals, and 3) silicate minerals. As discussed for sulphate and potassium, sewage pollution may have some relevance at the borehole scale.

The contents of atmospheric CO_2 in the sampled rainfall are between $10^{-3.61}$ atm and $10^{-3.25}$ atm (Fig. 8 left). Though the contents of CO_2 in shallow (3 to 10 m depth) and deeper (20 to 30 m depth) groundwater samples vary within a similar range, in the shallowest samples most of the values are between $10^{-3.3}$ atm and $10^{-2.6}$ atm, while in the deeper samples most of the values are between $10^{-3.7}$ atm and $10^{-3.3}$ atm. This suggests that dissolution of edaphic CO_2 by recharging groundwater is an active process across the basin, and that the consumption of CO_2 by mineral dissolution in the first 30 m of aquifer is not substantial. The last hypothesis is coherent with the fact that the calcite and dolomite saturation indexes increase very little, if they do, with depth (see Table 1), and also with the fact that almost all the samples at both depths are near equilibrium with calcite and dolomite (SI within ± 0.5). Thus, carbonate dissolution along groundwater flow in the saturated zone is not expected to be a great contributor of dissolved bicarbonate, though it can contribute to some extent.

Three deep samples with high CO_2 contents ($>10^{-3}$ atm) are from boreholes located in the lower basin (Fig. 8 left), where in humid periods rain water accumulates in the soil surface (where there is abundant vegetal and animal organic matter) and percolates through the annular space of the boreholes. Thus, the high CO_2 contents of some deep samples can be explained by rapid infiltration of surface water through the drilling space at flooding stages. Fig. 8 right provides more information on the main sources of CO_2 and HCO_3 across the basin: in the samples from the upper and middle sectors of the basin the CO_2 contents decrease as those of HCO_3 increase, whereas in the samples from the lower basin both the CO_2 and HCO_3 contents increase. This suggests that in the upper and middle basins the main source of bicarbonate is the dissolution of CO_2 and of solid carbonates, while in the lower basin the main source is organic matter decomposition, probably from soil humus and also from animal waste and farming wastewater.

With respect to the role of silicate (plagioclase) dissolution in contributing bicarbonate to groundwater, based on the above discussion and on the following statements, it is a minor one: i) as discussed previously, albite dissolution must occur mostly during rainwater infiltration through the unsaturated zone, and the thickness of this zone decreases to the lower basin, where the water table is quite shallow; ii) in the lower basin groundwater at the two study depths is oversaturated in albite (Fig. 6).

4.2.2.4. Sources of calcium. The main potential sources of calcium are carbonate and anorthite dissolution. As already mentioned, according to the calcite saturation indexes (Table 1) all the samples at the two

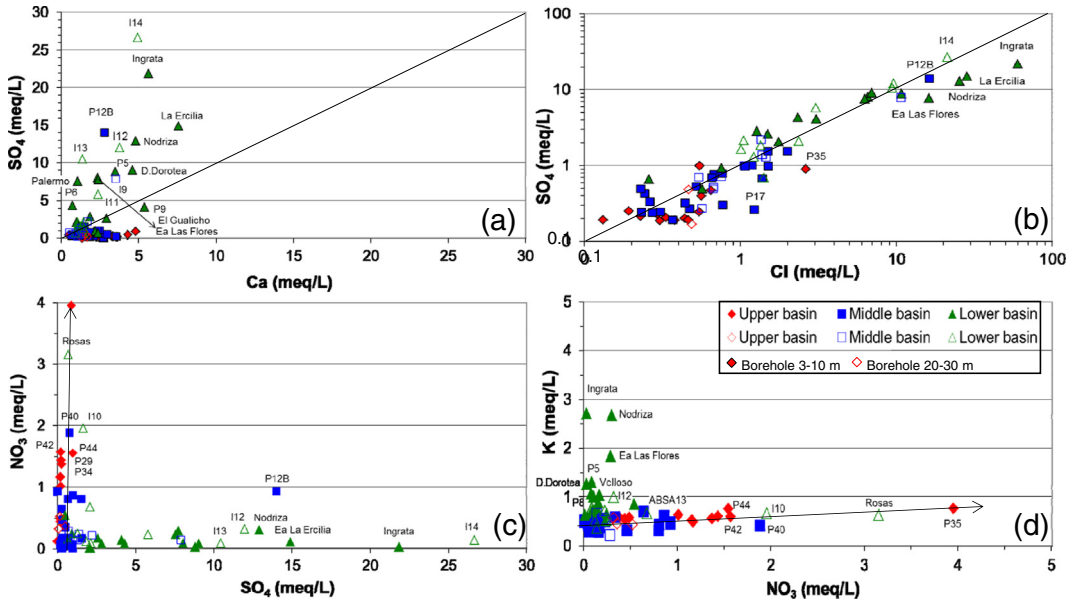

Fig. 7. Relationship between (a) sulphate and calcium contents, (b) sulphate and chloride contents, (c) sulphate and nitrate contents, (d) potassium and nitrate contents in samples from the two studied depths (3–10 m and 20–30 m).

study depths are close to equilibrium with that mineral, but calcite dissolution must happen mostly during groundwater recharge, and may be also at the top of the saturated zone. Concerning the possible dissolution of anorthite, a few samples are close to equilibrium but most of them are undersaturated at the two study depths (Table 1 and Fig. 6), which suggests that anorthite dissolution could also be a source of calcium. The activities of the chemical species resulting from the dissolution of anorthite (calculated by PHREEQC) point to the probable formation of Ca-montmorillonite as a result of this process (Fig. 6), and this is supported by the X-ray analyses of the clay-size fraction. Finally, as mentioned before when discussing Fig. 5, the content of Ca in groundwater is controlled by cation exchange with adsorbed Na.

4.2.2.5. Sources of magnesium. The main potential sources of magnesium are carbonate and silicate dissolution, evaporation and mixing with saline groundwater in the lower basin. The only Mg bearing mineral identified in the sediments analysed is dolomite, but other works mention the presence of pyroxenes within the Pampeano Formation (Teruggi and Kilmurray, 1975, 1980; Taboada, 2006). According to the dolomite saturation indexes (Table 1) most of the samples are close to equilibrium with dolomite, and only a few are oversaturated. This suggests that dolomite dissolution would occur mostly during groundwater recharge, and to a lesser extent once in the saturated zone, probably fostered by cationic exchange with sodium.

The occurrence of pyroxene dissolution cannot be checked with the information available. But the low solubility of silicates compared to carbonates, and the great effectivity of cation exchange inducing changes in the contents of cations in solution would make pyroxene dissolution a discrete source of magnesium. However, this aspect would merit a dedicated study, not yet performed. Finally, as for the rest of the major solutes, concentration by evaporation and mixing with already saline groundwater is the main cause of the relatively large concentrations of magnesium in the lower basin.

4.2.2.6. Sources of chloride. Chloride contents in groundwater at the two studied depths are quite similar and range between less than 10 mg/L and around 2000 mg/L in the available shallowest samples, and around 700 mg/L in the available deeper samples. The regional evolution is the same at both depths, with increasing values from the upper to the lower basin (Fig. 9). As described in Section 2.3, the main origin of chloride in groundwater of the Salado River lower basin is well known since some decades ago.

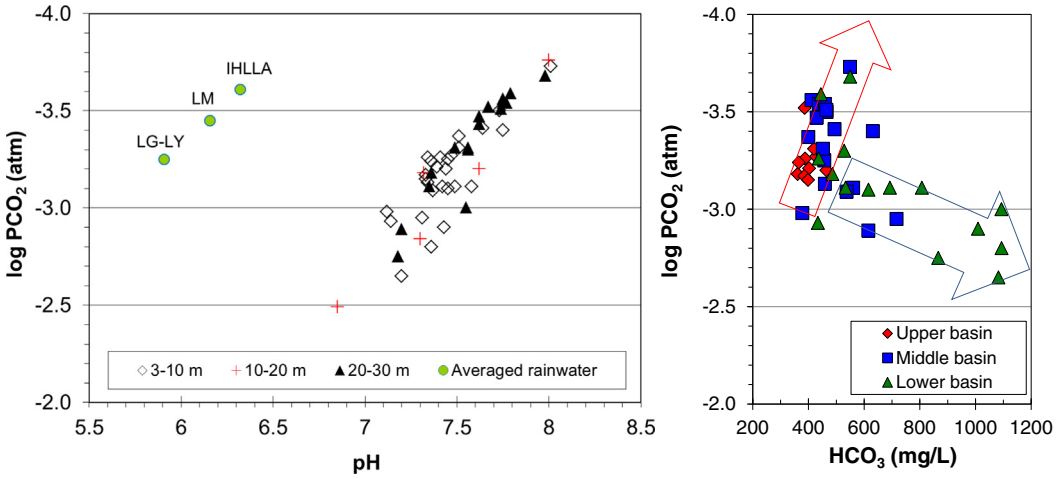

Fig. 8. Left: CO_2 content vs. pH in rainwater and groundwater. Right: Evolution of CO_2 and HCO_3 contents in the shallow groundwater samples (3–10 m depth).

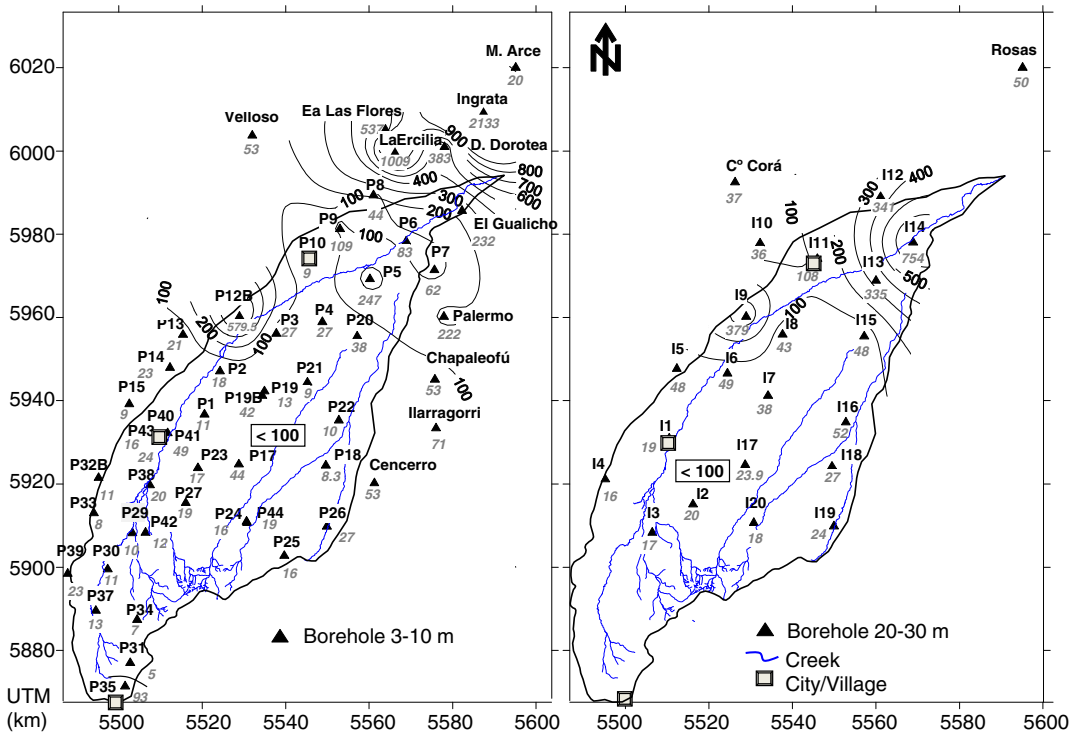

Fig. 9. Chloride content (mg/L) distribution in groundwater at the two study depths.

In this work, the existence of several sources of chloride in groundwater has been studied with the support of the ionic ratio Cl/Br (molar). The compilation of Cl/Br values performed by Alcalá and Custodio (2008) for many types of water having different salinity sources has been used as conceptual framework (Fig. 10). Three groups of samples were identified: 1) samples with Cl contents lower than 100 mg/L and Cl/Br values lower than that of sea water value (655 ± 4), whose salinity comes from the atmospheric contribution (even if it is concentrated by evaporation); 2) samples with Cl contents between ≈80 and 300 mg/L and Cl/Br values smaller than the sea water value, whose characteristics are consistent with an agricultural contribution of salinity; 3) samples with Cl contents between ≈50 and 1000 mg/L and Cl/Br values between the sea water value and 2000, whose characteristics are consistent with the contribution of salts from leaching of effluents generated by human activities (domestic/livestock). Besides the clear polluting effect of domestic waste water and garbage in some of the saltiest samples in the lower basin, evaporation of recharge water and mixing with the resident saline groundwater have to be considered as the main sources of salinity, and pollution by urban activities as an over-imposed source.

Therefore, the main sources of chloride in the basin are atmospheric supply, which is concentrated by evapotranspiration, and mixing with saline groundwater in the lower basin. A third source, not so relevant from the quantitative point of view but certainly important from the

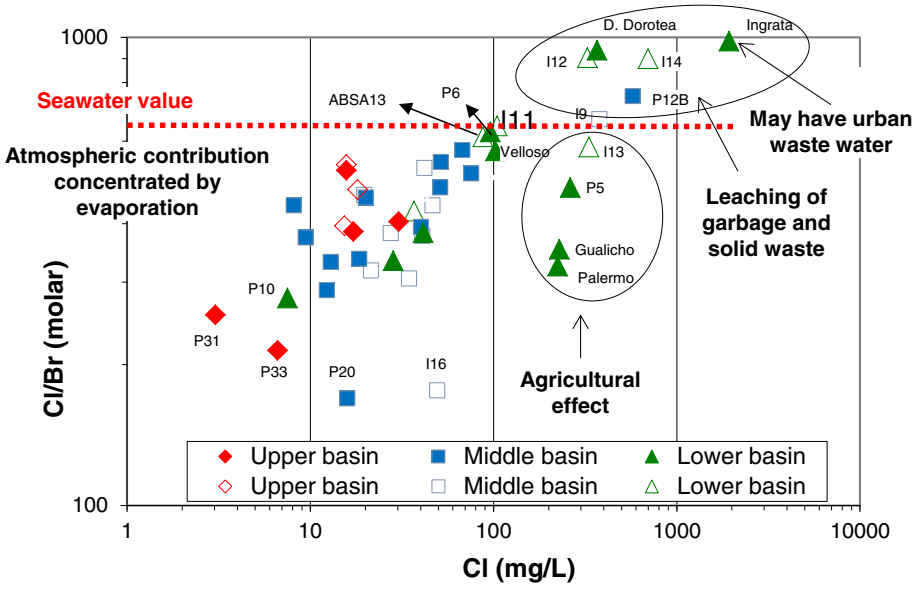

Fig. 10. Plot of Cl (mg/L) vs. Cl/Br (molar) at the two studied depths, 3–10 m and 20–30 m.

qualitative one, are human wastes. Infiltration of waste water and leaching of solid wastes are polluting groundwater across the basin. The concentrating effect of evaporation expands the signals of pollution.

4.2.3. Isotopic composition of groundwater and its origin

Fig. 11 shows the isotopic composition of groundwater at the two study depths. Also shown is the meteoric water line of the Azul city (Dapeña et al., 2010), which is located in the central-western part of the basin. This meteoric line may not represent the full range of values of the whole basin rainfall, but it is the closest reference. The figure shows that many samples from both study depths are below both the Azul city and the world meteoric water lines, and they are located along evaporation lines; thus evaporated groundwater is present at least as deep as 30 m. The figure also shows that many samples are coherent with the Azul city meteoric water line, however they show a wide range of variation for both isotopes (around two units for $\delta^{18}O$ and 40 units for $\delta^{2}H$ in the shallower samples; somewhat less in the deeper samples), which suggests that the isotopic signature of recharge water varies that much across the basin.

Other samples, mostly among the shallower ones, are above the Azul city meteoric water line. This could obey to two different reasons: either there was recharge after specific rainfall events not representative of the most common conditions in the basin, or they were recharged outside the basin. The second hypothesis is more feasible, as due to the nature of the aquifer (granular) it is not probable for groundwater at 5, 10 and 30 m depth to be the result of particular rainfall recharge.

At both depths groundwater isotopic composition ranges between −6.2 and −2.5‰ for $\delta^{18}O$ and between −40 and −18‰ for $\delta^{2}H$, although most of the samples are between −6 and −4 5‰ for $\delta^{18}O$ and between −37 and −24‰ for $\delta^{2}H$. Despite the wide ranges of variation, most of the non-evaporated, deeper samples (20–30 m) seem to concentrate around $\delta^{18}O \approx -5‰$ and $\delta^{2}H \approx -27‰$, but this can be the result of the smaller regional extension of the 30 m depth monitoring network.

The relationship between $\delta^{18}O$ and Cl was studied to assess groundwater salinity origin. Fig. 12 shows several groups of samples whose values can be explained by different salinization origin and processes. The composition of samples in group A is consistent with an atmospheric origin, and its range of concentrations can be explained by evaporation in different degrees, though not very intense in relative terms, while their salinity is due to leaching of soil water concentrated by evaporation or evapotranspiration in the upper and middle basins. The composition of samples in group B has also atmospheric origin, and their isotopic and Cl values are due to significant evaporation prior or during recharge in the middle and lower basin. The isotopic composition of samples in group C is coherent with evaporation in different degrees, while their salinity could be explained by leaching of strongly evaporated soil water and shallow groundwater in the middle basin. However,

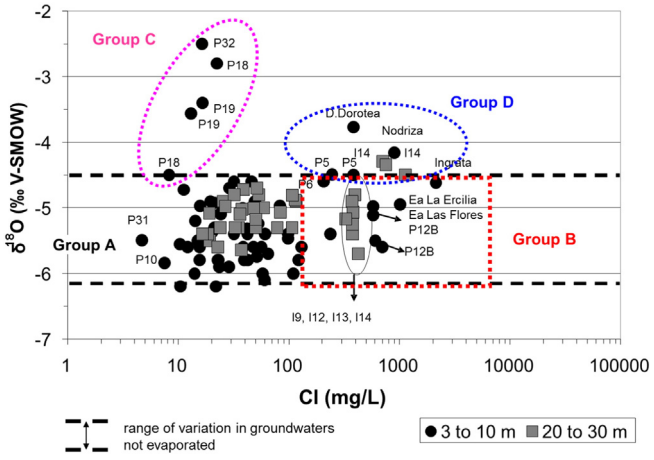

Fig. 12. Relationship between the Cl contents (mg/L) and the $\delta^{18}O$ values in the studied samples. See description of the groups in the text.

other chemical characteristics of some samples in this group, like Ingrata, Nodriza, Ea Las Flores, La Ercilia, and D. Dorotea (group D), point to the mixing of water with salinity of atmospheric origin and saline waste water, probably from the intense livestock activity existing in the area. Thus, the combined use of the ionic ratio Cl/Br, the stable isotopes and the chloride content allowed confirming that human activities are significant sources of pollution to groundwater, especially in the lower basin.

4.3. Hydrogeochemical modelling

According to the previous analysis about the possible main sources of solutes for groundwater in the upper 30 m of the Pampeano Aquifer in the DACB, the following two conceptual hydrogeochemical models were proposed to explain 1) which are the main processes controlling the incorporation of solutes to groundwater during rain water infiltration in the upper basin, and 2) the regional evolution of major solute contents along a regional horizontal flow path at around 30 m depth in the Pampeano Aquifer.

The main processes taking place during groundwater recharge in the upper basin would be:

- Dissolution of soil CO_2, anorthite, calcite and dolomite. In the upper basin carbonate minerals are not only part of the aquifer sediments, they are also supplied as dust particles carried by the wind from the nearby quarries.
- Cationic exchange of Ca and possibly Mg in solution by Na adsorbed.

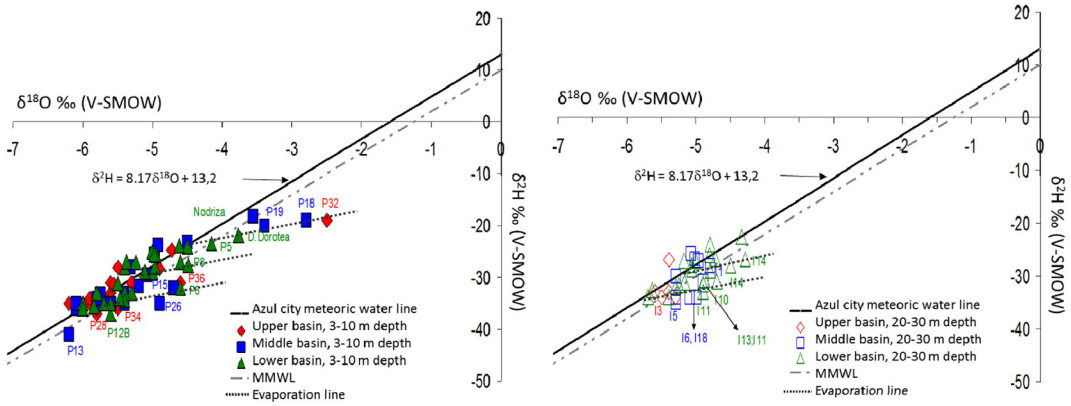

Fig. 11. Isotopic composition of groundwater of the Del Azul Creek basin. Left: Shallow samples (3 to 10 m depth). Right: 20–30 m depth samples.

Table 3
Mass balance (mmol/L) between average rain water in the upper basin (LY–LG station) concentrated by evapotranspiration and groundwater from the P31 borehole. FC: evapo-concentration factor.

	mmol/L									
	Ca	Mg	Na	K	Cl	NO_3	SO_4	HCO_3	SiO_2	Al_{tot}
Average rain water LY–LG	0.054	0.022	0.042	0.069	0.035	0.016	0.010	0.088	0.096	0.000004
Hypothetic recharge water (FC * $Cl_{rain\ water}$)	0.134	0.053	0.102	0.168	0.086	0.039	0.025	0.215	0.235	0.000009
P31 (June 2011)	1.143	1.405	2.577	0.560	0.086	0.047	0.095	3.561	2.182	0.000371
Mass balance P31 — hypothetic recharge	1.009	1.352	2.475	0.392	0	0.008	0.070	3.346	1.946	0.000362

$FC = Cl_{LY-LG} / Cl_{P31} = 2.457$.

– Precipitation of Ca-montmorillonite and silica (most probably as quartz).

Other dissolution and precipitation processes involving both carbonate (for example, magnesium calcite) and silicate (pyroxenes, micas, etc.) minerals may also occur, but if so they probably contribute very little to the contents and changes of the major components. Kaolinite precipitation has not been considered in view of the data shown in Fig. 6.

Moreover, as shown by the isotopic enrichment of shallow groundwater, in many places of the basin groundwater is notably concentrated with respect to rain water by evaporation before or during infiltration. This is clearly occurring in the middle and lower basin, where the conditions favor ponding of rain water, but to a lesser scale also in the upper basin. Thus, evapo-concentration has also been considered as a mechanism increasing solute contents in groundwater.

To check the thermodynamic feasibility of the former geochemical reactions, the possible main processes explaining the concentration differences between recharge water (rain water) from the LY–LG station already concentrated by evaporation/evapotranspiration and a very low mineralized groundwater sample from the same place (represented by the sample P31), have been modelled with PHREEQC. Previously to modelling, the evapo-concentration factor was calculated after the ratio between Cl content in borehole P31 and in average rain water of station LY–LG, and the hypothetical recharge water concentrated by evapotranspiration was calculated. The mass balance between both types of water is shown in Table 3 and Fig. 13 Left.

Bicarbonate content increases notably, followed by that of sodium and, in decreasing order, silica, magnesium and calcium. This means that, after concentration by evapotranspiration, the most effective processes incorporating solutes to groundwater during recharge should be dissolution of CO_2 and probably of carbonate minerals, cation exchange and subordinate silicate dissolution.

One of the possible sets of processes that can satisfy this mass balance and is coherent with the information available about aquifer mineralogy and mineral saturation indexes is shown in Table 4. Following this model, anorthite dissolution would provide all the necessary Ca to exchange with Na, and the dissolution of both minerals is quite probable in reality. Though this model does not consider the possible dissolution of albite as a second source of Na, this process is also very prone to occur during groundwater recharge, as the infiltrated rain water would be undersaturated with respect to albite.

Regarding the processes occurring along a flow path at 30 m depth, the main reactions would be:

– Cation exchange of adsorbed Na with Ca and Mg in solution.
– Anorthite dissolution.
– Ca-montmorillonite precipitation.

Kaolinite precipitation has not been considered in view of the data shown in Fig. 6. Calcite and dolomite dissolution may take place, as groundwater at 30 m is nearly in equilibrium with both minerals, but if so, they would incorporate into solution small quantities of Ca and Mg.

To check the thermodynamic feasibility of those processes, the possible reactions taking place during groundwater flow along a regional flow path at 30 m depth between the locations represented by boreholes I3 (upper basin) and I8 (middle to lower basin) was been modelled with PHREEQC. The mass balance between both types of water is shown in Table 5 and Fig. 12 (right). Sodium is the most increasing component, followed by bicarbonate, chloride and sulphate. Silica and magnesium increase far less than during groundwater recharge, and calcium decreases slightly. This suggests that the most effective processes modifying solute concentrations along groundwater flow at 30 m depth are cationic exchange and carbonate dissolution, probably induced by cation exchange. Dissolution of some silicates seems to take place too, but they seem to contribute very little to the changes of Ca, Mg, HCO_3 and Na contents as compared to the other two processes.

However, at 30 m depth there are neither sources nor processes to explain the chloride and sulphate increases, and the only possible process to account for them is mixing with more saline groundwater. This saline groundwater is the resident water of the aquifer, at least of the 30 uppermost metres, in this part of the basin, which means that steady

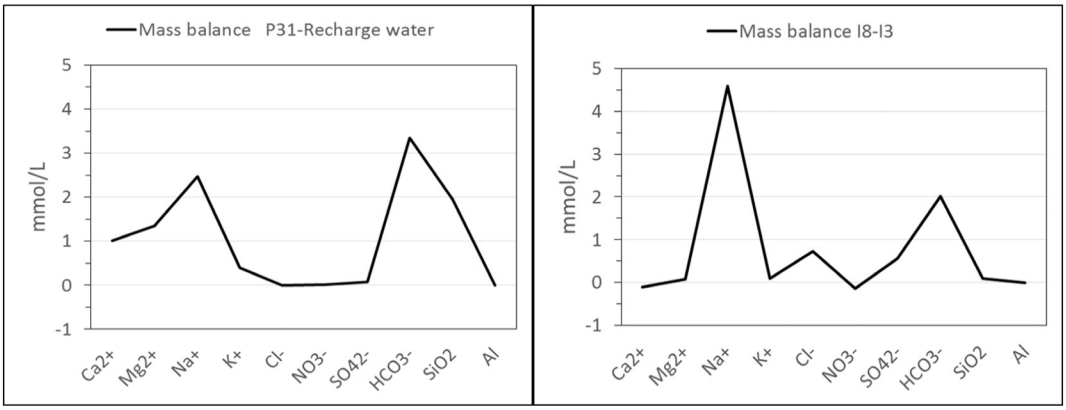

Fig. 13. Illustration of solute mass balances for the two conceptual models discussed. Left: Mass balance between rain water (concentrated by evapotranspiration) at the LY–LG station and shallow groundwater (borehole P31) in the upper basin. Right: Mass balance along a representative horizontal flow path at 30 m depth from the upper basin (borehole I3) to the lower basin (borehole I8).

Table 4
One of the thermodynamically feasible hydrogeochemical models calculated with PHREEQC to explain the changes in solute contents during groundwater recharge in the upper basin. Positive values mean dissolution or release by cation exchange; negative ones mean precipitation or uptake by cation exchange.

Phase	Composition	M1
CO_2		1.76E−03
Dolomite	$CaMg(CO_3)_2$	1.19E−03
Anorthite	$CaAl_2Si_2O_8$	1.36E−03
Ca-montmorillonite	$Ca_{0.165}Al_{2.33}Si_{3.67}O_{10}(OH)_2$	−1.92E−03
CaX_2		−1.24E−03
NaX		2.48E−03
SiO_2		2.95E−03

All quantities are in mol/kg.

evaporation has been a relevant process concentrating soil water and groundwater at least since some thousand years ago. Besides mixing with saline groundwater, the frequent presence of nitrate in boreholes of this depth suggests mixing with shallow, polluted groundwater. Due to the very smooth vertical gradients, this mixing is most probably occurring on a local scale than on a regional one, and as already suggested, it probably happens at borehole scale due to surface water infiltration through the annular space during the yearly flooding stages.

Assuming that the only cause to explain the compositional differences between groundwater from boreholes I3 and I8 is the occurrence of reactions during groundwater horizontal flow at 30 m depth, some of the several possible sets of processes than can satisfy the mass balance of Table 5 are shown in Table 6. Almost all the models are equally probable, except may be those that indicate the precipitation of K-feldspar (see the discussion on the sources of K above), though it is not impossible. As all the samples are oversaturated in albite, the only source for Na increase is cation exchange. With respect to that, it is important to note that even when the mass of Na transferred from the exchanger to the solution is the largest transfer process in all the models from a quantitative point of view, the mass of Na transferred according to PHREEQC calculations is far smaller than the one shown in Table 5 (2.97 mmol/L instead of 4.58 mmol/L). This is due to the fact that to perform successful inverse modelling with PHREEQC it was necessary to adjust the initial concentrations of both samples to an extent further than desirable. But even though the magnitudes are not reliable, the processes suggested by the models are absolutely feasible.

Both the groundwater composition observed in the DACB and the main chemical processes deduced to explain it are in agreement with those described by several authors in other areas of the Pampeano Aquifer (Logan and Nicholson, 1998; Logan et al., 1999; Martínez and Osterrieth, 1999, 2013; Miretzky et al., 2000, 2001; Kruse et al., 2010; Carol et al., 2012). However, though there is general agreement that the modelled short set of processes is the main cause of the observed regional groundwater chemistry in the Pampeano Aquifer, this study is the first to suggest that the major part of all the hydrogeochemical processes must occur in the unsaturated zone during groundwater recharge. Thus, from a quantitative point of view the contribution of those hydrogeochemical processes to groundwater mineralization along the flow through the aquifer is rather small compared to their contribution during recharge.

On the other hand, the generalized isotopic enrichment of groundwater in the uppermost 30 m of aquifer points to the concentration of atmospheric and lithology derived salts by evaporation and evapotranspiration as the most significant process controlling groundwater mineralization in the shallowest part of the saturated zone. This process must have been lasting during at least some thousands of years, until the construction during the 1990 decade of a network of channels to drain the endorheic plain located between the Tandilia Range and the Salado valley. Some authors mention weathering of secondary salts from Postpampeano sediment in areas to the north of the DACB (Gabellone et al., 2008), and some other allude to recurrent halite and gypsum precipitation and dissolution during dry and wet periods respectively in shallow temporary lagoons nearby the Salado River (Quirós et al., 2002). Those processes are coherent with the ionic contents and ratios observed in the lower DACB, though halite and gypsum have not been found in the mineralogical analysis performed. However, the sampling was neither extensive nor systematic, and it did not include the sediments of the lagoons. This is a subject to be studied in the future.

5. Conclusions

The chemical and isotopic compositions of groundwater at the two studied depths (3–10 m and 20–30 m) of the Pampeano Aquifer across the Del Azul Creek Basin, Argentina, are practically identical, and changes are observed only laterally, following the main regional horizontal flow paths from southwest to northeast. According to the studied samples from the first 30 m of Pampeano Aquifer, groundwater salinity increases down gradient from values around 600 μS/cm in the upper basin to values around 7500 μS/cm in the lower basin. In the upper basin groundwater is mostly of the HCO_3-Ca type, with some HCO_3–MgCa cases; in the middle basin it is of the HCO_3-Na type, and in the lower basin it is of the $ClSO_4$–NaCa and Cl–Na types.

Two conceptual models have been proposed to explain the most significant hydrogeochemical processes occurring across the basin and contributing solutes to groundwater. One of the models focuses on the main reactions taking place during groundwater recharge from rainwater, which produces HCO_3-Ca/Mg groundwater; the other focuses on the main reactions occurring along a flow path from the upper to the middle and lower basin at 30 m depth, which changes groundwater chemistry from HCO_3-Ca to HCO_3-Na. The thermodynamic feasibility of those two models has been validated by hydrogeochemical modelling. With respect to the conversion of HCO_3-Na into $ClSO_4$–NaCa and Cl–Na groundwater in the lower basin, though being a very relevant change it has not been modelled as it is not the result of geochemical reactions, but of physical processes, evaporation and mixing with already saline water. However, this will be the subject of future works.

The study of the processes that provide solutes to groundwater during rainwater recharge has been performed only in the upper basin because in the rest of the DACB ponding is frequent in the humid season and the evaporation rates are large, thus making the study difficult. According to validation of the proposed conceptual model with hydrogeochemical modelling, the main processes that increase groundwater mineralization during recharge in the upper basin are: rain water evaporation (in this zone, probably during infiltration), dissolution of CO_2, calcite, dolomite, silica, and to a lesser extent, anorthite and probably albite; cationic exchange with Na release and Ca and Mg uptake, and precipitation of clays, mostly Ca-montmorillonite.

Table 5
Mass balance between the chemical compositions of two samples from boreholes located along a regional flow path at 30 m depth. Borehole I3 is in the upper basin and borehole I8 is in the lower basin. Positive values mean increase of content along flow; negative ones mean decrease.

	mmol/L									
	Ca	Mg	Na	K	Cl	NO_3	SO_4	HCO_3	SiO_2	Al_{tot}
I3	0.840	0.516	4.319	0.434	0.486	0.261	0.083	6.333	2.167	0.000541
I8	0.739	0.600	8.904	0.527	1.222	0.121	0.643	8.341	2.269	0.000452
I8–I3	−0.101	0.084	4.584	0.092	0.736	−0.139	0.559	2.008	0.102	−0.00009

Table 6
Feasible sets of reactions or models (M) taking place during groundwater flow along a regional flow path at 30 m depth between the locations represented by boreholes I3 and I8.

Phase	Composition	M1	M2	M3	M4	M5	M6	M7
Calcite	$CaCO_3$	1.29E−03	6.40E−04		1.28E−03			1.28E−03
Dolomite	$CaMg(CO_3)_2$	−6.72E−06	−2.19E−05	6.29E−04		6.40E−04		
Anorthite	$CaAl_2Si_2O_8$	1.09E−05	1.09E−05	4.20E−05	1.09E−05		1.51E−03	
K-feldspar	$KAlSi_3O_8$	−2.19E−05			−2.19E−05			
Ca-montmorillonite	$Ca_{0.165}Al_{2.33}Si_{3.67}O_{10(}OH)_2$					−3.82E−08	−1.26E−03	−3.82E−08
Illite	$K_{0.6}Mg_{0.25}Al_{2.3}Si_{3.5}O_{10}(OH)_2$			−3.65E−05			−3.65E−05	
SiO_2		9.19E−05		9.19E−05	9.19E−05	4.82E−05	1.78E−03	4.82E−05
CaX_2		−1.49E−03	−8.38E−04	−8.58E−04	−1.48E−03	−8.27E−04	−1.49E−03	−1.47E−03
NaX		2.97E−03	2.97E−03	2.97E−03	2.97E−03	2.97E−03	2.97E−03	2.97E−03
MgX_2			−6.47E−04	−6.27E−04	−6.72E−06	−6.58E−04	2.41E−06	−1.77E−05

All quantities are in mol/kg.

The hydrogeochemical model proposed to explain the chemical changes observed between the upper and the middle and lower basins along horizontal flow paths at 30 m depth consist of: cationic exchange with Na release and Ca and Mg uptake, dissolution of silica, anorthite (and may be some calcite and dolomite), and precipitation of Ca-montmorillonite (probably also Na-montmorillonite) and may be illite. However, the proposed processes cannot explain the significant increase of sulphate and chloride contents along flow from the upper to the middle and lower basins. Following the information provided by the isotopic data ($\delta^{18}O$ and $\delta^{2}H$), the main origin of salinity in the middle and lower basins is evaporation, which has been a relevant process concentrating soil water and groundwater at least since some thousand years ago.

With respect to groundwater pollution by human activities, the information provided by the NO_3 contents and the Cl/Br ratio values points to the existence of several sources of pollution, mostly from agricultural and domestic activities and from cattle rising. Agricultural pollution affects groundwater mostly in the upper and middle sectors of the basin, but also to locations of the lower basin. Many of the studied samples from the lower basin are not polluted, which is coherent with the prevalent shallow water table in this area and with the existence of saline groundwater at least until 30 m depth. However, both the Cl/Br ratio and the NO_3 contents (as large as 20 mg/L) show that some of the most saline samples are polluted by domestic waste water and/or by leaching of garbage. Diffuse pollution is not expected to occur widely in the middle and the lower basin due to the reasons described above, but it can happen at a borehole-scale. Borehole pollution can take place by preferential flow of contaminated surface and shallow groundwater through the annular space of the borehole, which is favoured by the water table drawdown observed in urban areas (due to pumping of deeper layers for water supply) and by the frequent flooding episodes.

Future works related with this study should focus on the mechanisms of groundwater pollution, the existence and location of natural remediation conditions, and the confection of cartography on groundwater quality which could be used for management.

Acknowledgements

This research was supported by the "Dr. Eduardo J. Usunoff" Large Plain Hydrology Institute (IHLLA, Argentina) and the project REDESAC (CGL2009-12900-C03-03), funded by the Spanish Ministry of Economy and Innovation. The first author was funded by the Consejo Nacional de Investigaciones Científicas y Técnicas (CONICET-Argentina). We thank the IHLLA technical staff for their assistance in carrying out the chemical analyses and water sampling. We also thank Dr. Daniel Martinez (Universidad Nacional de Mar del Plata, Argentina) for carrying out the isotopic analysis of rainwater, and Dr. Daniel Poiré (Universidad Nacional de La Plata, Argentina) for performing the mineralogical analysis. Also, we want to express our gratitude to all the well owners for their positive attitude, which is very much appreciated. Finally, the authors are indebted to five anonymous reviewers whose observations and recommendations contributed largely to improve this work.

References

Aceñolaza, F.G., 2000. La Formación Paraná (Mioceno medio): estratigrafía, distribución regional y unidades equivalentes. In: Aceñolaza, F.G., Herbst, R. (Eds.), El Neógeno de Argentina. Serie de Correlación Geológica 14. INSUGEO, San Miguel de Tucumán, pp. 9–27.

Alcalá, F.J., Custodio, E., 2008. Using Cl/Br ratio as a tracer to identify the origin of aquifers in Spain and Portugal. J. Hydrol. 359, 189–207.

APHA, 2005. Standard Methods for the Examination of Water and Wastewater. 21st ed. APHA-AWWA-WEF, Washington, D.C.

Argañaráz, J.P., Entraigas, I., 2010. Análisis de los tipos de cubierta del suelo en la Cuenca baja del Arroyo del Azul (Buenos Aires, Argentina) a partir de imágenes Landsat 5 TM. In: Varni, M., Entraigas, I., Vives, L. (Eds.), Hacia la Gestión Integral de los Recursos Hídricos en Zonas de Llanura. Editorial Martín, Mar del Plata, pp. 623–630.

Auge, M.P., Strelczenia, V.B., 1990. Características hidrogeológicas de Azul, provincia de Buenos Aires, República Argentina. VI Congreso Brasileño de Aguas Subterráneas, Puerto Alegre, pp. 72–81.

Auge, M.P., Hernández, M., Hernández, L., 2002. Actualización del conocimiento del acuífero semiconfinado Puelche en la provincia de Buenos Aires, Argentina. In: Bocanegra, E., Martinez, D., Massone, H. (Eds.), Groundwater and Human Development. UNdMP, Mar del Plata, pp. 624–633.

Bonorino, A.G., Limbozzi, F., Albouy, R., Lexow, C., 2008. Movilidad de metales y otros elementos en el acuífero loéssico regional del suroeste bonaerense. Geoacta 33, 31–42.

Carol, E.S., Kruse, E.E., Laurencena, P.C., Rojo, A., Deluchi, M.H., 2012. Ionic exchange in groundwater hydrochemical evolution. Study case: the drainage basin of El Pescado creek (Buenos Aires province, Argentina). Environ. Earth Sci. 65 (2), 421–428.

Coleman, M.L., Sheperd, T.J., Durham, J.J., Rouse, J.E., Moore, F.R., 1982. A rapid and precise technique for reduction of water with zinc for hydrogen isotope analysis. Anal. Chem. 54, 993–995.

Custodio, E., Manzano, M., 2008. Groundwater quality background levels. In: Quevauviller, P. (Ed.), Groundwater Science and Policy. An international Overview. The Royal Society of Chemistry, Cambridge, pp. 193–216.

Dalla Salda, L., Spalletti, L., Poiré, D., De Barrio, R., Echeveste, H., Benialgo, A., 2006. Tandilia. Ser. Correl. Geol. 26 (1), 65–74.

Dangavs, N., 2009. Los paleoambientes cuaternarios del arroyo La Horqueta, Chascomús, provincia de Buenos Aires. Rev. Asoc. Geol. Argent. 64 (2), 249–262.

Dangavs, N., Blasi, A., 2002. Los depósitos de yeso intrasedimentario del arroyo El Siasgo, partidos de Monte y General Paz, Provincia de Buenos Aires. Rev. Asoc. Geol. Argent. 57 (3), 315–327.

Dapeña, C., Varni, M., Panarello, H.O., Ducos, E., Weinzettel, P., Usunoff, E., 2010. Composición isotópica de la precipitación de la Estación Azul, provincia de Buenos Aires. Red Nacional de Colectores Argentina. In: Varni, M., Entraigas, I., Vives, L. (Eds.), Hacia la Gestión Integral de los Recursos Hídricos en Zonas de Llanura. Editorial Martín, Mar del Plata, pp. 386–393.

Daughney, C.J., Meilhac, C., Zarour, H., 2009. Spatial and temporal variations and trends in groundwater quality in the Manawatu-Wanganui region. GNS Science Report 2009/02. GNS Science, Lower Hutt, p. 137.

Edmunds, W.M., Shand, P., 2008. Natural Groundwater Quality. Blackwell Publishing Ltd., Oxford, UK, pp. 71–91.

Edmunds, W.M., Shand, P., Hart, P., Ward, R.S., 2003. The natural (baseline) quality of groundwater: a UK pilot study. Sci. Total Environ. 310 (1–3), 25–35.

Entraigas, I., Varni, M., Gandini, M., Usunoff, E., Vázquez, P., 2004. Inundación y Anegamiento. In: Gonzáles, M.A., Bejerman, N.J. (Eds.), Peligrosidad Geológica en Argentina. Metodologías de Análisis y mapeo. Estudio de casos. Editorial Asociación Argentina de Geología Aplicada a la Ingeniería, Córdoba, pp. 230–246.

Fidalgo, F., De Francesco, F.O., Pascual, R., 1975. Geología superficial de la llanura bonaerense (Argentina). VI Congreso Geológico Argentino. Geología de la Provincia de Buenos Aires. Asociación Geológica Argentina, Bahía Blanca, pp. 103–138.

Frenguelli, J., 1950. Rasgos generales de la morfología y la geología de la provincia de Buenos Aires. 33. Laboratorio de Ensayo de Materiales e Investigaciones Tecnológicas, pp. 1–72 (Serie 2).

Frenguelli, J., 1955. Loess y Limos Pampeanos. Serie Técnica y Didáctica 7. Facultad de Ciencias Naturales y Museo de La Plata, p. 88.

Gabellone, N.A., Solari, L.C., Claps, M.C., Neschuk, N.C., 2008. Chemical classification of the water in a lowland river basin (Salado River, Buenos Aires, Argentina) affected by hydraulic modifications. Environ. Geol. 53 (6), 1353–1363.
González Bonorino, F., 1965. Mineralogía de las fracciones arcilla y limo del Pampeano en el área de la ciudad de Buenos Aires y su significado estratigráfico y sedimentológico. Rev. Asoc. Geol. Argent. 20 (1), 67–148.
González Bonorino, F., Zardini, R.A., Figueroa, M., Limousin, T., 1956. Estudio Geológico de las Sierras de Olavarría y Azul. Provincia de Buenos Aires. Rev. An. LEMIT 63, 5–23 (Serie II).
Haynes, R.J., Williams, P.H., 1993. Nutrient cycling and soil fertility in the grazed pasture ecosistema. Adv. Agron. 49, 119–199.
Heredia, O.S., Santa Cruz, J.N., Fernández Cirelli, A., 2003. Procesos en la Zona No Saturada: intercambio catiónico en el agua del suelo. III Congreso Argentino de Hidrogeología y I Seminario Hispano-Latinoamericano sobre temas actuales de la hidrología subterránea, Rosario, Santa Fe 1, pp. 169–177.
Hernández, M.A., Giaconi, L.M., González, N., 2002. Línea de base ambiental para las aguas subterráneas y superficiales en el área minera de Tandilia. Buenos Aires, Argentina. In: Bocanegra, E., Martínez, D., Massone, H. (Eds.), Groundwater and human development. Editorial International Association of hydrogeologists, Mar del Plata, pp. 336–343.
Holzman, M.E., Rivas, R., Piccolo, M.C., 2013. Estimating soil moisture and the relationship with crop yield using surface temperature and vegetation index. Int. J. Appl. Earth Obs. Geoinf. 28, 181–192.
IHLLA, 1996. Red de monitoreo de las aguas subterráneas en la cuenca del arroyo del Azul. Final report. Instituto de Hidrología de Llanuras, Azul (Bs As), p. 73 (Internal report).
IHLLA, 2005. Hidrogeología de los sectores alto y medio de la cuenca del arroyo Azul. Informe final. Final report. Instituto de Hidrología de Llanuras, Azul (Bs As), p. 306 (Internal report).
IHLLA, 2008. Herramientas para la gestión sustentable de los recursos hídricos en una cuenca de llanura. Final report. Instituto de Hidrología de Llanuras, Azul (Bs As), p. 220 (Internal report).
Iriondo, M., Kröhling, D., 2007. Geomorfología y sedimentología de la cuenca superior del río Salado (sur de Santa Fe y noroeste de Buenos Aires, Argentina). Lat. Am. J. Sedimentol. Basin Anal. 14 (1), 1–23.
Krishan, G., Lapworth, D.J., Someshwar Rao, M., Kumar, C.P., Smilovic, M., Semwal, P., 2014. Natural (baseline) groundwater quality in the Bist-Doab catchment, Punjab, India: a pilot study comparing shallow and deep aquifers. Int. J. Earth Sci. Eng. 7 (1), 16–26.
Kruse, E., Carol, E., Deluchi, M., Laurencena, P., Rojo, A., 2010. Hidroquímica subterránea en un sector de la zona deprimida del Salado, Prov. de Bs As. I Congreso de Internacional de Hidrología de Llanuras, Azul, Bs. As, pp. 414–419.
Lis, G., Wassenaar, L.I., Hendry, M.J., 2008. High-precision laser spectroscopy D/H and $^{18}O/^{16}O$. measurements of microliter natural water samples. Anal. Chem. 80, 287–293.
Loeppert, R., Suárez, D.L., 1996. Carbonate and gypsum. Publication from USDA-ARS/UNL Faculty. Paper 504; Available from:. http://digitalcommons.unl.edu/usdaarsfacpub/504.
Logan, W.S., Nicholson, R.V., 1998. Origin of dissolved groundwater sulphate in coastal plain sediments of the Río de La Plata, eastern Argentina. Aquat. Geochem. 3, 305–328.
Logan, W.S., Auge, M.P., Panarello, H.O., 1999. Bicarbonate, sulfate, and chloride water in a shallow, clastic-dominated coastal flow system, Argentina. Groundwater 37 (2), 287–295.
Manzano, M., Zabala, M.E., 2012. El fondo químico natural del sistema acuífero de la cuenca del río Matanza-Riachuelo. Proyecto de Aguas Subterráneas en la Cuenca Matanza Riachuelo. [cited 2014 Oct 14]; Informe 5. p. 221. Available from:. http://www2.acumar.bdh.org.ar:8081/bdh3/publicacion_master.php?idobject=15107&retorno=publicacion_listado.php.
Manzano, M., Custodio, E., Nieto, P., 2003. El fondo natural de la calidad del agua subterránea. I Seminario Hispano-Latinoamericano sobre temas actuales de la Hidrología Subterránea, Rosario, pp. 607–620.
Manzano, M., Custodio, E., Iglesias, M., Lozano, E., 2008. Groundwater baseline composition and geochemical controls in the Doñana aquifer system (SW Spain). In: Edmunds, W.M., Shand, P. (Eds.), Natural Groundwater Quality. Blackwell Publishing, USA, UK, Australia, pp. 216–232.
Marengo, H.G. Micropaleontología y estratigrafía del Mioceno marino de la Argentina: Las transgresiones de Laguna Paiva y del "Entrerriense-Paranense" (Ph. D thesis) UBA; 2006. p. 124. Unpublished.
Martínez, D.E., Osterrieth, M., 1999. Geoquímica de la sílice disuelta en el Acuífero Pampeano en la Vertiente Sudoriental de Tandilia. II Congreso Argentino de Hidrogeología, San Miguel de Tucumán 13, pp. 241–250.
Martínez, D.E., Osterrieth, M., 2013. Hidrogeoquímica y efectos de la contaminación en un acuífero en sedimentos loéssicos cuaternarios en el área de rellenos sanitarios de Mar del Plata, Argentina. Rev. Fac. Ing. Univ. Antioquia 66, 9–23.
Martínez, D., Osterrieth, M., Maggi, J., 1998. Equilibrio solución-fase mineral en el acuífero clástico de la cuenca superior del arroyo Lobería, Partido de General Pueyrredón. V Jornadas Geológicas y Geofísicas Bonaerenses, Mar del Plata 2, pp. 23–30.
Migueltorena, M.V., Entraigas, I., D'Álfonso, C., Scaramuzzino, R., 2009. Introducción al estudio de los bajos dulces y alcalinos de la cuenca del arroyo del Azul (Buenos Aires). II Jornadas Argentinas de Ecología de Paisajes, Córdoba, p. 60.
Miretzky, P., Conzonno, V., Fernández, Cirelli A., 2000. Hydrochemistry of pampasic ponds in the lower stream bed of Salado River drainage basin, Argentina. Environ. Geol. 39 (8), 951–956.
Miretzky, P., Conzonno, V., Fernández, Cirelli A., 2001. Geochemical processes controlling silica concentrations in groundwaters of the Salado River drainage basin, Argentina. J. Geochem. Explor. 73 (3), 155–166.
Morgenstern, U., Daughney, C.J., 2012. Groundwater age for identification of baseline groundwater quality and impacts of land-use intensification—The National Groundwater Monitoring Programme of New Zealand. J. Hydrol. 456/457, 79–93.
Nieto, P., Custodio, E., Manzano, M., 2005. Baseline groundwater quality: a European approach. Environ. Sci. Pol. 8, 399–409.
NRCS-USDA, 2004. Soil survey laboratory methods manual. Soil Survey Investigations Report N° 42, Version 4.0.
Panarello, H.O., Parica, C.A., 1984. Isótopos del oxígeno en hidrogeología e hidrología. Primeros valores en aguas de lluvia de Buenos Aires. Rev. Asoc. Geol. Argent. 39 (1–2), 3–11.
Parkhurst, D.L., Appelo, C.A., 1999. User's guide to PHREEQC, a computer program for speciation, reaction path, advective-transport, and inverse geochemical calculations. Water Resources Investigation Report. US Geological Survey, pp. 99–4259.
Quirós, R., Rennella, A., Bovery, J.J., Sosnovsky, A., 2002. Factores que afectan la estructura y funcionamiento de las lagunas pampeanas. Ecol. Austral 12, 175–185.
Quiroz Londoño, O.M., Martínez, D.E., Dapeña, C., Massone, H., 2008. Hydrogeochemistry and isotope analyses used to determine groundwater recharge and flow in low-gradient catchments of the province of Bs As, Argentina. Hydrogeol. J. 16 (6), 1113–1127.
Robert, M., Tessier, D., 1974. Méthodes de préparation des argiles des sols pour les études minéralogiques. Ann. Agron. 25 (6), 859–882.
SAGyP. Mapas de suelos de la provincia de Buenos Aires. Escala 1:500000. INTA. CIRN 1989.
Sala, J.M., Kruse, E., Aguglino, R. Investigación hidrogeológica de la Cuenca del arroyo Azul, Provincia de Buenos Aires. Unpublished technical report, Comisión de Investigaciones Científicas, La Plata; 1987. p. 235.
Santa Cruz, J.N., 1972. Estudio sedimentológico de la formación Puelches en la Provincia de Buenos Aires. Rev. Asoc. Geol. Argent. XXVI (1), 5–62.
Shand, P., Edmunds, W.M., Lawrence, A.R., Smedley, P.L., Burke, S., 2007. The natural (baseline) quality of groundwater in England and Wales. British Geological Survey Research Report N° RR/07/06 and Environment Agency Technical Report NC/99/74/24, p. 72.
Taboada, M.A., 2006. Soil structural behavior in flooded and agricultural soils of the Argentine Pampas. (Ph.D). Institut National Polytechnique de Toulouse, p. 361.
Tardy, Y., 1971. Characterization of the principal wheathering types by the geochemistry of waters from some European and African crystalline massifs. Chem. Geol. 7, 253–271.
Teruggi, M., 1957. The nature and origin of the Argentine loess. J. Sediment. Petrol. 27 (3), 322–332.
Teruggi, M., Kilmurray, J., 1975. Tandilia. Relatorio del VI Congreso Geológico Argentino, Bs. As, pp. 55–77.
Teruggi, M., Kilmurray, J., 1980. Sierras Septentrionales de la Provincia de Buenos Aires. II Simposio de Geología Regional Argentina, Córdoba II, pp. 919–966.
Thorez, J., 2000. Modes operatoires pour la préparation des échantillons et l'analyse minéralogique qualitative et semi-quantitative par diffraction des rayons x de materiaux et de minérux argileux destinés à la confection de barrières argileuses. Manuel relatif aux matières naturelles pour barrières argileuses ouvragées pour C.E.T. (centres d'enfouissement technique) et réhabilitation de dépôtoirs en Région wallonne. Ministère de la Région wallone, Direction générale des Ressources naturelles et de l'Environnement, Bélgica (Available from: http://environnement.wallonie.be/rapports/owd/barrieres_argileuses/manuel.htm#_Toc487693207).
Tófalo, O.R., Etchichury, M.C., Fresina, M., 2005. Características texturales y petrofacies de depósitos neógenos, Bancalari, provincia de Buenos Aires. Rev. Asoc. Geol. Argent. 60 (2), 316–326.
Usunoff, E., Arias, D., 2004. Reactividad de solutos comunes en aguas subterráneas de la cuenca del arroyo del Azul, Argentina. Rev. Latinoam. Hidrogeología 4, 67–70.
Usunoff, E., Varni, M., 1995. Hidrología de los sectores alto y medio de la cuenca del arroyo Azul. Technical Report. Instituto de Hidrología de Llanuras, Azul, p. 315.
Usunoff, E., Varni, M., Arias, D., Rivas, R., Weinzettel, P., 1995. Equilibrio químico en el acuífero freático de la cuenca del arroyo del Azul, provincia de Buenos Aires. IV Jornadas Geológicas y Geofísicas Bonaerenses, Junín II, pp. 247–254.
Usunoff, E.J., González Castelain, J., Arias, D., 2003. Variación de la calidad del acuífero del Azul (Provincia de Buenos Aires, Argentina) por efectos locales. I Seminario Hispano-Latinoamericano Sobre Temas Actuales de la Hidrología Subterránea, Rosario II, pp. 423–431.
Varni, M., Usunoff, E., 1999. Simulation of regional-scale groundwater flow in the Azul River Basin, Buenos Aires Province, Argentina. Hydrogeol. J. 7 (2), 180–187.
Varni, M., Comas, R., Weinzettel, P., Dietrich, S., 2013. Application of the water table fluctuation method to characterize groundwater recharge in the Pampa plain, Argentina. Hydrol. Sci. J. http://dx.doi.org/10.1080/02626667.2013.833663.
Weinzettel, P., Varni, M., Zabala, M.E., Dietrich, S., 2009. Diseño de pozos de muestreo en un sector de la cuenca baja del arroyo del Azul, Provincia de Buenos Aires. In: Mariño, E., Schulz, C. (Eds.), Aportes de la Hidrogeología al conocimiento de los Recursos Hídricos. Amerindia Nexo di Nápoli, Santa Rosa, pp. 229–238.
Wendland, F., Blum, A., Coetsiers, M., Gorova, R., Griffioen, J., Grima, J., et al., 2008. European aquifer typology: a practical framework for an overview of major groundwater composition at European scale. Environ. Geol. http://dx.doi.org/10.1007/s00254-007-0966-5.
Wilcox, J.D., Bradbury, K.R., Thomas, C.L., Bahr, J.M., 2005. Assessing background ground water chemistry beneath a new unsewered subdivision. Groundwater 43 (6), 787–795.
Zabala, M.E. Actualización del modelo conceptual y zonificación hidroquímica del acuífero de la cuenca del arroyo del Azul (M.Sc thesis) UNLPam; 2009. p. 158. Unpublished.
Zabala, M.E. El origen de la composición química del acuífero freático en la cuenca del arroyo del Azul (Ph.D thesis) UNC; 2013. p. 490. Unpublished.
Zabala, M.E., Weinzettel, P., Varni, M., 2006. Utilización de ensayos de pulso para la estimación de la conductividad hidráulica en la Cuenca del arroyo del Azul, Provincia

de Buenos Aires, Argentina. VIII Congreso Latinoamericano de Hidrología Subterránea, Asunción, Paraguay, pp. 95–96.
Zabala, M.E., Manzano, M., Vives, L., 2010. Estudio preliminar del origen del fondo químico natural de las aguas subterráneas en la cuenca del arroyo del Azul. In: Varni, M., Entraigas, I., Vives, L. (Eds.), Hacia la Gestión Integral de los Recursos Hídricos en Zonas de Llanura. Editorial Martín, Mar del Plata, pp. 249–256.
Zabala, M.E., Manzano, M., Varni, M., Weinzettel, P., 2011. On the sources of salinity in groundwater under plain areas. Insights from 18O, 2H and hydrochemistry in the Azul River basin, Argentina. Proceedings International Symposium on Isotopes in Hydrology, Marine Ecosystems, and Climate Change Studies, Mónaco 1, pp. 287–294.
Zabala, M.E., Manzano, M., Vives, L., 2014. Estudio del origen de la composición química del agua del acuífero Pampeano en la cuenca del Arroyo del Azul (Buenos Aires). In: Venturini, V., Rodríguez, L., Cello, P., et al. (Eds.), Memorias del II Congreso Internacional de Hidrología de Llanuras. Universidad Nacional del Litoral, Santa Fe (CD ROM).